HYSTERETIC BEHAVIOUR OF A SIMPLE CHARGE DENSITY WAVE SYSTEM

by

Mustafa Mert Terzi

B.S, Mechanical Engineering, Boğaziçi University, 2011

Submitted to the Institute for Graduate Studies in
Science and Engineering in partial fulfillment of
the requirements for the degree of
Master of Science

Graduate Program in Physics

Boğaziçi University

2013

ACKNOWLEDGEMENTS

First and foremost, I am grateful to Muhittin Mungan, for accepting me as his student and for sharing this exciting thesis topic with me. I would like to thank him also for everything that he taught me, both within and outside physics. He has and still continues to impress me with his great knowledge, his enthusiasm for physics, and his kindness and understanding.

My decision to study physics was largely influenced by Tonguç Rador's relativity class that I took as an undergraduate. I would like to thank him for this, as well as for everything I learned in his graduate level classes.

I would like to thank Tonguç Rador and Atilla Yılmaz for being part of my defense jury.

I would also like to thank Teoman Turgut and Ali Kaya, for all the great classes they teach.

Needless to say, I would like to express my gratitude to my mother, my father and my brother, for all the support they showed throughout this process.

I wish to thank Lâle for making all the distances bearable.

I am lucky to have Gizem, Bilal and Cem as my classmates, and I am grateful to them for not leaving me alone through all the time we spent in the library.

I would like to thank İdil, Ilgım and Osman for standing by me and for everything else that I can't even begin to tell here.

I would like to thank all the members of Muhittin Mungan's research group for valuable discussions.

ABSTRACT

HYSTERETIC BEHAVIOUR OF A SIMPLE CHARGE DENSITY WAVE SYSTEM

In this thesis, the hysteretic behaviour in a simple 1D Charge Density Wave (CDW) system is investigeted. Such systems can be represented as elastically coupled particles in a periodic potential with a random phase-offset in the presence of a uniform external force. CDWs are models for depinning transitions: for a force smaller then a threshold force, all configurations are static, while a sliding dynamic behavior is obtained when the threshold force is exceeded. The systems we consider have two unique and distinct threshold configurations, corresponding to reaching the threshold via positive and negative force increments. We study how hysteresis occurs in between these two threshold configurations. For a fixed system size, there is a finite number of pinned states that can be obtained by arbitrarily varying the external force while keeping the system in the pinned configuration. We find a power law relation between system size L and the total number of reachable states which are the configurations that can be reached from the threshold configurations by sequence of increasing or decreasing forces. We also observe that our model has the return-point memory effect.

ÖZET

BASİT BİR YÜK YOĞUNLUĞU DALGA MODELİNİN HİSTERESİS DAVRANIŞI

Bu tezde, bir boyutlu Yük Yoğunluğu Dalga modelinde histeresis davranışları araştırıldı. Bu tür sistemler periodik potansiyel içinde birbirleriyle elastik etkileşimde bulunan ve rastgele faza sahip parçacıklar ile temsil edilirler. Bu sistemler ayrıca her parçacık üzerine aynı ektide bulunan bir dış kuvvet ile sürülürler. Yük Yoğunluğu Dalgaları statik durumdan dinamik duruma geçiş modelleridir. Eşik kuvvetinden küçük kuvvetler için bütün konfigürasyonlar statiktir ve bu eşik kuvvetinden büyük kuvettlerde dinamik davranış elde edilir. Bizim incelediğimiz sistemler sadece iki tane eşik konfigürasyonuna sahiptir. Bu iki eşik konfigürasyonu pozitif ve negatif kuvvet uygulanarak elde edilir. Burada bu konfigürasyonlar arasındaki histeresis davranışlarının nasıl oluştuğu incelendi. Sabit bir sistem boyutu için kuvveti değiştirerek elde edilebilecek sonlu sayıda statik konfigürasyon vardır. Eşik kuvvetinden başlayarak bir dizi kuvvet uygulayıp erişilebilinen konfigürasyonlar erişilebilinir konfigürasyonlardır. Sistemin boyutu L ve erişilebilinir konfigürasyonlar arasında bir kuvvet yasası bulduk. Ayrıca modelimizde dönüş noktası hafızası özelliği gözlemledik.

TABLE OF CONTENTS

ACKNOWLEDGEMENTS iii
ABSTRACT iv
ÖZET v
LIST OF FIGURES viii
LIST OF TABLES x
LIST OF SYMBOLS xi
LIST OF ACRONYMS/ABBREVIATIONS xii
1. INTRODUCTION 1
2. THE MODEL 5
2.1. The Toy Model 11
2.1.1. Threshold Configurations 12
2.1.2. Threshold to Threshold Evolution of the Toy Model with $S = 1$ 14
2.1.3. The Rank Representation of a Configuration 17
2.1.4. Example: Threshold to Threshold Evolution 19
2.1.5. ZFA Evolution and the Rank Representation for General S . . . 23
2.1.6. The Active Region 23
3. THE DISTRIBUTION OF THE NUMBER OF AVALANCHES IN THE THRESHOLD TO THRESHOLD EVOLUTION 25
3.1. Determining $P(N|i, \pi(k^-))$ 28
3.2. Determining $P_L(N)$ 31
3.2.1. Comparison with Numerical results 33
3.2.2. Determining $\mathbb{E}N$ 34
4. HYSTERESIS BEHAVIOUR 37
4.1. Force Cycles and Hysteresis Loops 37
4.2. The Reachable states 40
4.3. Description of the Numerical Algorithm 41
4.4. Numerical Results 42
4.4.1. Partial Ordering and Hierarchies 44
5. CONCLUSION 46

APPENDIX A: RECORD STATISTICS AND STIRLING NUMBERS 47
A.1. Some Useful Identities Involving Stirling Numbers 51
A.2. Intermediate Steps leading from Equation A.24 to Equation 3.32 52
REFERENCES 59

LIST OF FIGURES

Figure 1.1. The plot of an hysteresis loop of a two dimensional CDW model with size 64^2. The hysteresis loop starts from the negative threshold field and the system is driven to the positive threshold field and then back to the negative threshold field [1]. 2

Figure 1.2. Figure taken from [2]. This loop shows the return-point memory effect for a random field Ising model with system size 30^3. See text for details. 4

Figure 2.1. The piece-wise parabolic pinning potential, Equation 2.2. The unit cell extends from $x = -1/2$ to $x = 1/2$. 5

Figure 3.1. Lines correspond to Equation 3.32 for five different system size L. The dots give the distribution of the total number of steps in the threshold to threshold evolution obtained from numerical simulations. The number of realizations is given in parentheses next to their corresponding L. 33

Figure 4.1. The representation of the hysteresis loop that contains the negative and the positive threshold configurations. In the figure every circle represents a distinct state such that $1, 2, 3, 4$ and 5 represents the configurations 4.3, 4.5, 4.4, 4.6 and 4.7, respectively. The black and the red arrows represent transitions. 40

Figure 4.2. The reachability graph of our example showing all reachable states and the transitions between them. The red (black) arrows indicate transitions under applying the ZFA once in the positive (negative) direction. 43

Figure 4.3. Numerically obtained relation between the system size and the average of the total number of reachable states on a log-log scale (blue data points). The red line is a power-law with exponent 3/2. . . . 44

Figure 4.4. The reachability graph for a system of size $L = 32$. 45

LIST OF TABLES

Table 4.1. This is the initial state of our pointer vector. 42

Table 4.2. This table shows the final state of our algorithm. It contains all reachable states and the transitions between them. 42

LIST OF SYMBOLS

F	External driving force
$\mathcal{H}$	Hamiltonian
i	Level
j_L	The left end of an avalanche
j_R	The right end of an avalanche
J_i	Defect on site i
k^-	Defect site that ensures integer well numbers at the negative threshold configuration
k^+	Defect site that ensures integer well numbers at the positive threshold configuration
ℓ	Size of active Region
L	System size
m_i	Well number of site i
N	The number of steps
S	Total topological charge
y_i	Coordinate of site i
$\tilde{y}_i$	Well coordinate of site i
z	Rescaled well coordinate of site i
α_i	Random phase at site i
Δ	Discrete Laplacian
ζ_i	Generalization of ω_i for $S \neq 1$
η	Attenuation factor
λ	Strength of the potential
$\pi(i)$	Permutation that order the ζ_i
σ_i	Permutation that order the ω_i
ω_i	Difference between Laplacian of phases and nearest integer of laplacian of phases

LIST OF ACRONYMS/ABBREVIATIONS

CDW	Charge density wave
FLR	Fukuyama-Lee-Rice
ZFA	Zero force algorithm

1. INTRODUCTION

Charge Density Waves (CDW) are elastic media that are driven by an external force in the presence of random impurities. CDWs exhibit a depinning transition which occurs when the applied force exceeds a threshold force. Once the threshold force is exceeded, the CDW system starts to slide. Fisher has argued that the deppining transition exhibited by CDW sis a dynamical critical phenomenon [3, 4]. In other words, the deppinning transition is a phase transition in which the external force is the control parameter. Fisher has also shown that the threshold behaviour has similar features of a second order phase transition such as the breakdown of perturbation theory, existence of scaling laws and critical exponents near threshold. This is the reason why such transitions are referred to as a dynamical critical phenomenon.

The deppining transition allows us to observe both a static and dynamic regime. Using the Fukuyam-Lee-Rice Hamiltonian as a simple CDW model, [5,6], work has been done both for the dynamic and pinned behaviour of CDWs. For example, Fisher and Middleton used the Fukuyama-Lee-Rice Hamiltonian in order to study the threshold behaviour, as approached from both the pinnned and sliding state [1, 3, 4]. The FLR Hamiltonian is given by,

$$\mathcal{H} = \frac{1}{2}\sum_{(i,j)}(y_j - y_i)^2 - h\sum_{i=1}^{N}\cos(y_i - \alpha_i) - F(t)\sum_{i=1}^{L} y_i, \tag{1.1}$$

where y_i are the phases that lie on the linear, square or cubic lattice and α_i are the random impurities. The first sum in Equation 1.1 is over nearest neighbours that gives the elastic forces between sites. The second term represents the pinnig effect of the random impurity phases on the CDW. Middleton and Fisher have also shown that the threshold field is unique and that the threshold configuration is almost always unique. They use a key property of their model, the no-passing rule, in order to prove the uniqueness of the threshold. The no-passing rule states that if one configuration is "greater" than a second one in the sense that the phase of the first configuration is

greater than the corresponding phase of the second configuration at each site, it will always remain greater [1].

History dependent behaviour of a physical system is called hysteresis. This occurs for example if some external effect changes the state, shape or some other physical properties of a system and this change can not be fully recovered by the removal of that external effect. Therefore, the system remembers the change even after the removal of the external effect. We are interested in the static behaviour of CDW systems in this thesis.

Fisher has shown for the CDW systems that below the threshold there exists a large number of metastable stationary states and their selection depends of the function $F(t)$, which depends on history [4]. Middleton and Fisher also observed hysteretic behaviour in CDW systems via numerical simulations.

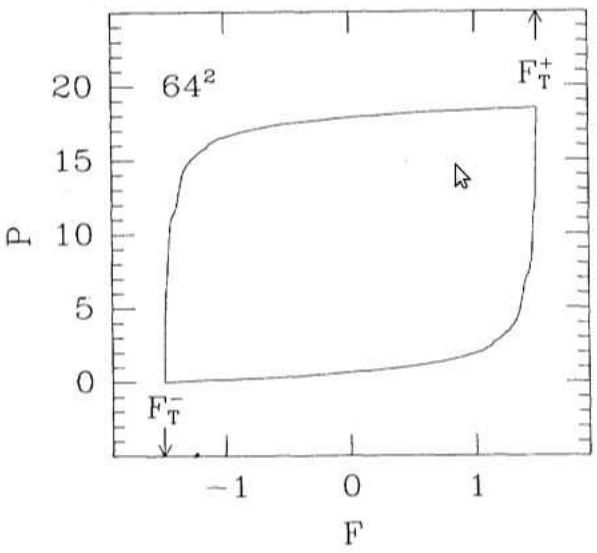

Figure 1.1. The plot of an hysteresis loop of a two dimensional CDW model with size 64^2. The hysteresis loop starts from the negative threshold field and the system is driven to the positive threshold field and then back to the negative threshold field [1].

When a sufficiently large driving force is exerted, the CDW can transit into a nearby metastable state. After the removal of the driving force the system does not

necessarily transit back into its initial configuration. Middleton and Fisher have also numerically obtained the hysteresis loop in the sub-threshold region [1]. Figure 1.1 shows such a hysteresis loop (from [1]).

Some hysteresis loops have the return-point memory effect: A system returns to its initial state after a proper evolution or a hysteresis loop, if it has return-point memory property. In other words, the system has a memory of its previous states. The states of the system that show return-point memory effect also form hierarchies in between them: This means that information of history can be saved only for bigger hysteresis loops. When the system is driven out of that hysteresis loop it also erases the memory of it. Sethna *et al.* [2] have shown that the zero temperature random-field Ising model exhibits a return-point memory effect. The return-point memory effect is demonstrated in Figure 1.2. The system returns to the same state after a hysteresis loop. The return-point memory effect allows the system to behave history dependent. As is seen in Figure 1.2, when we increase the applied magnetic field the system goes from A to B through a. If the applied magnetic field is decreased when the system is at B it goes down to C passing through b. If we continue to apply appropriate sequence of magnetization we end up at D. The return-point memory effect states that if the system is at D and we increase the magnetization, the system transits exactly to B. In other words, all states on the hysteresis loop that contain B and C and all states in that loop have a memory of B. Each state in this hysteresis loop, must pass through B if the system is driven out of this loop.

Let us give a very common example for a system that does not have the return-point memory effect: bending a metal beam. If we apply a force such that bends a metal beam to yield, it can not recover its initial shape after the removal of the force. We should apply a force opposite to the first one in order for the beam to recover its initial shape. This is how hysteresis can be observed in metal beams. However if we repeat this process many times the beam eventually fractures due to fatigue. On the other hand, systems that have hysteresis loops with return-point memory property can undergo the same hysteresis loops infinitely many times.

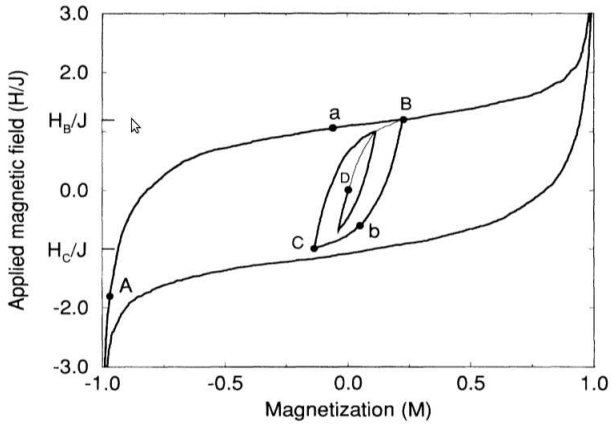

Figure 1.2. Figure taken from [2]. This loop shows the return-point memory effect for a random field Ising model with system size 30^3. See text for details.

Sethna *et al.* have shown [2] that the return-point memory effect can be explained by using the no passing rule that was introduced by Middleton and Fisher [1]: A system exhibits return-point memory effect if it has a partial ordering among its states, the no-passing property and evolves adiabatically.

If one solution of a system is greater than some other solution for all times we can say that this system is partially ordered. Landsberg and Friedman discussed the dynamical effects of partial ordering and they show [7] that CDW system are partially ordered.

This thesis is organized as follows. In Chapter 2 we introduce a toy model for a CDW system and discuss its evolution from the negative to the positive threshold configuration. This evolution process occurs by transitions through intermediate configuration via avalanches. In Chapter 3 we derive an exact expression for the distribution of the number of intermediate states, or equivalently, the number of avalanches triggered, during the evolution from one threshold configuration to the other. In Chapter 4 we consider the hysteretic behaviour of our toy model. We conclude this thesis with a discussion of our results. We have compiled material relevant to Chapter 3 in an Appendix.

2. THE MODEL

Our model consists of elastically coupled particles in a periodic potential with random phase offset. We drive the system with an external force F. The Hamiltonian of our model is a simplified version of the Fukuyama Lee Rice Hamiltonian [5, 6], Equation 1.1, but with a different potential written as,

$$\mathcal{H}(\{y_i\}) = \sum_i \frac{1}{2}\left(y_i - y_{i-2}\right)^2 + V\left(y_i - \alpha_i\right) - F y_i. \tag{2.1}$$

We require the pinning potential $V(x)$ to be periodic $V(x) = V(x+1)$ and choose it as

$$V(x) = \frac{\lambda}{2}(x - [\![x]\!])^2 \tag{2.2}$$

where λ is the pinning strength and $[\![x]\!]$ is the nearest integer to x. Figure 2.1 is a plot of $V(x)$.

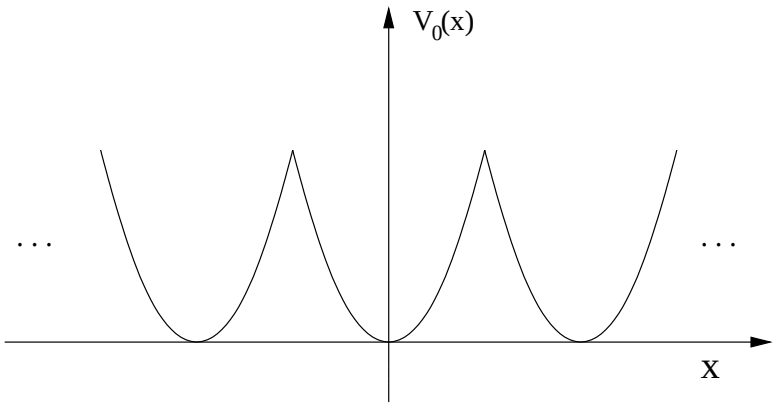

Figure 2.1. The piece-wise parabolic pinning potential, Equation 2.2. The unit cell extends from $x = -1/2$ to $x = 1/2$.

The α_i are random impurity phases and we assume that they are uniform *i.i.d.* on $\left(-\frac{1}{2}, \frac{1}{2}\right)$. In addition we impose periodic boundary conditions, $y_i = y_{i+L}$, where L is the system size.

The static behaviour of this model was investigated by Kaspar and Mungan in [8]. Static Solutions of Equation 2.2 correspond to $\{y_i\}$ which satisfy

$$\partial_i \mathcal{H} \equiv \frac{\partial \mathcal{H}}{\partial y_i} = 0, \tag{2.3}$$

for all i. So we can write,

$$0 = y_{i+1} - 2y_i + y_{i-1} + \lambda(y_i - \alpha_i - [\![\lambda(y_i - \alpha_i]\!]) + F. \tag{2.4}$$

Let us introduce the *well numbers* , m_i, and *well coordinates*, $\tilde{y}_i$,

$$m_i \equiv [\![y_i - \alpha_i]\!] \text{ and } \tilde{y}_i \equiv y_i - \alpha_i - m_i, \tag{2.5}$$

where the well number, m_i indexes the well in which the i^{th} particle is located, while the well coordinates, $\tilde{y}_i$, gives the relative coordinate of that particle with respect to the bottom of the potential well $\tilde{y}_i = 0$, *cf.* Figure 2.1. Therefore, m_i is an integer and $\tilde{y}_i \in \left(-\frac{1}{2}, \frac{1}{2}\right)$.

The solution of Equation 2.4,is given by,

$$y_i = \frac{1-\eta}{1+\eta} \sum_j \sum_n \eta^{|i-j+nL|}(\alpha_j + m_j + F/\lambda). \tag{2.6}$$

where the sum over n for all integer values, $n = \{0, \pm 1, \pm 2, \pm 3...\}$. The nL term comes from the periodic boundary condition. We choose L is large so that η^{nL} terms can be neglected. Therefore, y_i is given by

$$y_i = \frac{1-\eta}{1+\eta} \sum_j \eta^{|i-j|}(\alpha_j + m_j + F/\lambda). \tag{2.7}$$

where

$$\frac{1}{\eta} + \eta = 2 + \lambda \tag{2.8}$$

and

$$0 < \eta < 1 \tag{2.9}$$

is the smaller root of Equation 2.8.

Note that

$$\frac{1-\eta}{1+\eta} \sum_j \eta^j = 1. \tag{2.10}$$

Equation 2.7 can be rewritten using the well coordinates, $\tilde{y}_i$, as

$$\tilde{y}_i = \frac{\eta}{1-\eta^2} \sum_j \eta^{|i-j|} (\Delta\alpha_j + \Delta m_j) + F/\lambda. \tag{2.11}$$

Thus given the random impurities, α_i, and well numbers, m_i, we can determine the well coordinates from Equation 2.11. However, we require a self-consistency condition, namely, the set of well numbers, m_i and the external force F must be such that the well coordinates resulting from Equation 2.11 satisfy

$$\tilde{y}_i \in \left(-\frac{1}{2}, \frac{1}{2}\right). \tag{2.12}$$

With this restriction, the well numbers m_i and the force F together specify a static solution for our model.

One simple configuration can be found readily. Set $m_i = 0$ and $F = 0$ and suppose

this is a static configuration, that is, a solution of Equation 2.5. The compatibility condition Equation 2.12 restricts the admissible values of η. For $m_i = 0$ we have $\tilde{y}_i = y_i - \alpha_i$ Using Equation 2.7, we write,

$$y_i - \alpha_i = \frac{-2\eta}{1+\eta}\alpha_i + \frac{1-\eta}{1+\eta}\sum_{j\neq i}\eta^{|i-j|}\alpha_j, \tag{2.13}$$

which should satisfy Equation 2.12,

$$-\frac{1}{2} < y_i - \alpha_i < \frac{1}{2}, \tag{2.14}$$

and thus

$$-\frac{1}{2} < \frac{-2\eta}{1+\eta}\alpha_i + \frac{1-\eta}{1+\eta}\sum_{j\neq i}\eta^{|i-j|}\alpha_j < \frac{1}{2}. \tag{2.15}$$

Let us choose α_i in order to make $\tilde{y}$ maximum:

$$\alpha_l = \begin{cases} -1 \text{ if } l = i \\ 1 \text{ otherwise.} \end{cases} \tag{2.16}$$

and we find

$$\eta < \frac{1}{3} \quad \Leftrightarrow \quad \lambda > \frac{4}{3}\,. \tag{2.17}$$

We therefore see that given any α_i, we have a solution $m_i = 0$ and $F = 0$, if η satisfy Equation 2.17. For the sake of simplicity we will assume that Equation 2.17 is satisfied.

We investigate next the behaviour of our system under increase and decrease of the driving force, F. We assume that the dynamics of the particles is purely relaxational and that the force changes are sufficiently slow. As a result, the system can be assumed

to be in equilibrium configurations throughout the process.

What happens when we increase the force? At first, all particles translate uniformly,

$$\tilde{y}_i \to \tilde{y}_i + F/\lambda. \tag{2.18}$$

This conutinues until until a particle k reaches the cusp of the potential, $\tilde{y}_k = 1/2$ and thus the condition on the well coordinates, Equation 2.12, is violated. The first particle k to reach the cusp is the one that has maximum initial well coordinate,

$$k = \arg\max_i \tilde{y}_i. \tag{2.19}$$

If we increase the force further by an infinitesimally small amount, particle k jumps in to the the next well,

$$m_k \to m_k + 1. \tag{2.20}$$

The Laplacians of well numbers change accordingly,

$$\Delta m_k \to \Delta m_k - 2 \text{ and } \Delta m_{k\pm1} \to \Delta m_{k\pm1} + 1. \tag{2.21}$$

Therefore, change in the coordinates of particles due to the jump of particle k becomes,

$$\tilde{y}_j \to \tilde{y}_j - \delta_{k,j} + \frac{1-\eta}{1+\eta}\eta^{|j-k|}. \tag{2.22}$$

One can easily see that the effect of the jump of particle k on the other particles j decreases exponentially with the distance $|k-j|$ from that particle.

Since the jump of a particle advances the well-coordinates of its neighbouring particles, this can cause other particles to jump as well: after the jump of particle k, the well-coordinates of all other particles j are updated according to Equation 2.22. If the well coordinate of any one of them exceeds $\frac{1}{2}$, we must repeat the update process and an avalanche occurs. More precisely, an avalanche is the sequence of jumps of one or more particles which is triggered by the inital jump of a particle. Our system transits into another static configuration by avalanches.

When we continue to increase the force, new configurations are obtained by the triggering of avalanches. After a finite number of avalanches we reach a threshold configuration: this is the configuration with the property that if we increase the force by an additional infinitesimal amount, the resulting avalanche forces all particles translate by one well. We say that in this case the configuration has *depinned*.

Note that from Equation 2.10, it is clear that the jump of all particles is equivalent to a rigid translation by one well, $\tilde{y}_i \to \tilde{y}_i$.

As Kaspar and Mungan showed in [8], this model has both reversible and irreversible behaviour. All particles translate uniformly with the external driving force. If none of them changes wells, our system behaves *reversibly*. But if at least one of the particles changes wells, our system behaves *irreversibly*. When we increases the force and let a particle jump, this can trigger an avalanche. At any rate, the system goes into another static configuration that satisfies Equation 2.11. It can be shown that if we decrease the force back to zero, none of the particles jumps back.

We therefore see that *irriversibility* give rise to two important behaviours:

(i) It causes hysteretic behaviour of the system.
(ii) It enables us to write every static configuration in terms of an equivalent configuration with zero force, $F = 0$.

From (ii) we see that every configuration can be written in a way that differs only

by a rigid translation of its well number from an equivalent configuration with $F = 0$, *i.e.* the well coordinates for both configurations are the same.

Using this equivalence, we can without loss of generality restrict ourselves to the $F = 0$ versions of the configurations. In this case Kaspar and Mungan have shown that the evolution towards threshold under increasing driving force, can be represented interms of the equivalent *Zero-Force (ZF) configurations* via the zero force algorithm, ZFA:

(i) Find $k =$ arg $\max_i \tilde{y}_i$ and set $\tilde{y}_{max} = \tilde{y}_k$
(ii) Let $m_k \to m_k + 1$
(iii) Calculate new $\tilde{y}_i$, using Equation 2.22
If there is any $\tilde{y}_j$ such that $\tilde{y}_j > \tilde{y}_{max}$, set $k = j$ and go step 2.

For any static configuration this algorithm finds the sequence of static configuration that our system takes on as the driving force is increased.

2.1. The Toy Model

Kaspar and Mungan, [8] also introduced a toy model which is the small η (large λ) limit of the full model. In the toy model, we neglect the $O(\eta^2)$ terms so the well coordinates, Equation 2.11 can be written as,

$$\tilde{y}_i = \eta(\Delta\alpha_i + \Delta m_i), \tag{2.23}$$

in their equivalent zero force representation. The effect of the jump of one particle, Equation 2.22, in this limit now becomes, assuming that k jumps,

$$\tilde{y}_k \to \tilde{y}_k - 2\eta, \tag{2.24}$$

$$\tilde{y}_{k\pm1} \to \tilde{y}_{k\pm1} + \eta. \tag{2.25}$$

If we rescale the well coordinates as,

$$z_i \equiv \tilde{y}_i/\eta, \tag{2.26}$$

Equation 2.11 is given by,

$$z_i = \Delta\alpha_i + \Delta m_i, \tag{2.27}$$

and we can rewrite Equation 2.24 and Equation 2.25 as,

$$z_k \to z_k - 2 \text{ and } z_{k\pm1} \to z_{k\pm1} + 1, \tag{2.28}$$

where adding and subtracting of indices is mod L due to the periodic boundary condition such that $z_i = z_{i+L}$.

Hence, the zero force algorithm for the toy model becomes,

(i) Find $k =$ arg $\max_i z_i$ and set $z_{max} = z_k$
(ii) Let $m_k \to m_k + 1$, and calculate the new z_i using Equation 2.28
$z_k \to z_k - 2$
$z_{k\pm1} \to z_{k\pm1} + 1$.
(iii) If there is any z_j such that $z_j > z_{max}$, set $k = j$ and go to step (ii)

2.1.1. Threshold Configurations

Kaspar and Mungan also showed in [8] that, for given α_i, the threshold configuration can be found directly, *i.e.* without using ZFA: it turns out that finding the threshold configuration and solving the variational problem $\min_m \max_i z_i$ are equivalent. If we choose $\Delta m_i = -[\![\Delta\alpha_i]\!]$ then Equation 2.27, z_i becomes,

$$z_i = \Delta\alpha_i - [\![\Delta\alpha_i]\!]. \tag{2.29}$$

We know that m_i are integers for all i, so that Δm_i must have the following properties,

$$\sum_i \Delta m_i = 0, \tag{2.30}$$

$$\sum_i i\Delta m_i = 0 \text{ (mod L)}, \tag{2.31}$$

we will refer to the second condition as the divisibility condition. However, $\Delta m_i = -[\![\Delta\alpha_i]\!]$ does not necessarily satisfy Equation 2.30 and Equation 2.31. Therefore, we must modify the solution as follows:

$$\Delta m_i = -[\![\Delta\alpha_i]\!] + \gamma_i, \tag{2.32}$$

and Equation 2.30 and Equation 2.31 imply that,

$$\sum_i -[\![\Delta\alpha_i]\!] + \gamma_i = 0 \tag{2.33}$$

$$\sum_i i(-[\![\Delta\alpha_i]\!] + \gamma_i) = 0 \pmod{\text{L}}. \tag{2.34}$$

The choice of γ_i must be such as to yield $\min_m \max_i z_i$.

Define

$$S = \sum_{i=0}^{L-1} [\![\Delta\alpha_i]\!]. \tag{2.35}$$

Then given S, the positive threshold configuration can be written as,

$$\Delta m_i^+ = -[\![\Delta\alpha_i]\!] + J_i^+ - \delta_{i,k^+}, \tag{2.36}$$

where J_i^+ is determined as follows:

(i) For $S \geq 0$, $J_i^+ = 1$ for the $S+1$ different i where $\Delta\alpha_i - [\![\Delta\alpha_i]\!]$ have smallest value,

(ii) For $S < 0$, $J_i^+ = -1$ for $|S| - 1$ different i where $\Delta\alpha_i - [\![\Delta\alpha_i]\!]$ have largest value.

And we add -1 to another site, k^+, which is calculated by the divisibility condition, Equation 2.34, as

$$k^+ = \sum_{i=0}^{L-1} i(-[\![\Delta\alpha_i]\!] + J_i^+)(\mathrm{mod}L). \tag{2.37}$$

Notice that the system has also a negative threshold configuration m_i^- that is obtained by decreasing F. This configuration is obtained as a solution to the variational problem $\max_m \min_i z_i$, whose solution can be related to the postive threshold configuration of a system with phases $\alpha_i \to -\alpha_i$ with S as defined above. We find

$$\Delta m_i^- = -[\![\Delta\alpha_i]\!] + J_i^- + \delta_{i,k^-}, \tag{2.38}$$

where J_i^- is determined as follows:

(i) For $S \geq 0$, $J_i^- = 1$ for the $S - 1$ different i where $\Delta\alpha_i - [\![\Delta\alpha_i]\!]$ have smallest value,

(ii) For $S < 0$, $J_i^- = -1$ for $|S| + 1$ different i where $\Delta\alpha_i - [\![\Delta\alpha_i]\!]$ have largest value.

We add another $+1$ to the site, k^-, which is calculated by the divisibility condition, Equation 2.34, as

$$k^- = \sum_{i=0}^{L-1} i(-[\![\Delta\alpha_i]\!] + J_i^-)(\mathrm{mod}L). \tag{2.39}$$

2.1.2. Threshold to Threshold Evolution of the Toy Model with $S = 1$

Consider the case $S = 1$. The positive threshold configuration can be found as

(i) $J_i^+ = 1$ for $S + 1 = 2$ different i values where $\Delta\alpha_i - [\![\Delta\alpha_i]\!]$ is smallest,

(ii) Add -1 to site k^+, where k^+ is given in Equation 2.37.

The negative threshold configuration is calculated as

(i) $J_i^- = 1$ for $S - 1 = 0$ different i value so $J_i^+ = 0$ for all i,

(ii) Add 1 to site k^-, where k^- is given by Equation 2.39

$$k^- = \sum_{i=0}^{L-1} i(-[\![\Delta\alpha_i]\!]) \mathrm{mod} L). \tag{2.40}$$

Therefore we can write the negative threshold configuration for the $S = 1$ as

$$m_i^- = -[\![\Delta\alpha_i]\!] + \delta_{i,k_-}, \tag{2.41}$$

and z_i^- becomes,

$$z_i^- = \Delta\alpha_i - [\![\Delta\alpha_i]\!] + \delta_{i,k^-}. \tag{2.42}$$

Let us also define

$$\omega_i \equiv \Delta\alpha_i - [\![\Delta\alpha_i]\!]. \tag{2.43}$$

From the definition it follows that

$$\omega_i \in \left(-\frac{1}{2}, \frac{1}{2}\right), \tag{2.44}$$

and the well coordinates of the negative threshold configuration in the case $S = 1$, can be written as,

$$z_i^- = \omega_i + \delta_{i,k_-}. \tag{2.45}$$

Let us start out with the negative threshold configuration and increase the force F. From the ZFA, we see that the first site that will jump is k^-. Therefore in step (i) of the ZFA $z_{\max} = z_{k^-}$. Let particle k^- jump, after the jump we add -2 to site k^- and 1 to sites $k^- \pm 1$ for the step (ii). The well coordinates become

$$z_i = \omega_i - \delta_{i,k^-} + \delta_{i,k^-\pm 1}. \tag{2.46}$$

Now check whether $z_{k^-\pm 1}$ is greater than z_{max}. We know that $z_{k^-\pm 1} = \omega_{k^-\pm 1} + 1$ and $z_{max} = \omega_{k^-} + 1$, so we need to check if $\omega_{k^-\pm 1}$ is greater than ω_{k^-}. If ω_{k^--1} is greater than ω_{k^-} then particle $k^- - 1$ jumps. Likewise, if ω_{k^-+1} is greater than ω_{k^-} then $k^- + 1$ jumps as well. Next, suppose that both of them jump. Then we update the well coordinates as

$$\begin{aligned}
z_{k^--1} &\to z_{k^--1} - 2,\\
z_{k^-} &\to z_{k^-} + 1,\\
z_{k^--2} &\to z_{k^--2} + 1,\\
z_{k^-+1} &\to z_{k^-+1} - 2,\\
z_{k^-} &\to z_{k^-} + 1,\\
z_{k^-+1} &\to z_{k^-+1} + 1.
\end{aligned}$$

Therefore, the well coordinates become

$$z_i = \omega_i + \delta_{i,k^-} - \delta_{i,k^--1} - \delta_{i,k^-+1} + \delta_{i,k^--2} + \delta_{i,k^-+2}. \tag{2.47}$$

One can see that $z_{k^-} = z_{\max}$ again, so it jumps again, and well coordinates becomes

$$z_i = \omega_i - \delta_{i,k^-} + \delta_{i,k^--2} + \delta_{i,k^-+2}. \tag{2.48}$$

After the jump of k^-, we need to check whether z_{k^-+2} or z_{k^--2} is greater than $z_{\max}$. As one can see, the sequence of jumps will spread to both left and right until it reaches a site i such that $\omega_i < \omega_{k^-}$. We call these sites termination sites and refer to the

corresponding sequence of jumps as an avalanche wave. Suppose that our termination sites are i_L and i_R. These are the left and right ends of our first avalanche wave, respectively.

2.1.3. The Rank Representation of a Configuration

Before proceeding further let us introduce the rank diagrams. Observe that we actually do not need to real values of ω_i. The relative ranking of the ω_i is enough to determine sequence of jumps of the avalanche processes.

As we mentioned above, given any realization of random phases, the minimum and maximum elements of ω_i differ by less than one and we know that the minimum change that can be applied to a well coordinates during an avalanche is 1. Therefore

$$\omega_j + 1 > \omega_i \text{ and } \omega_j - 1 < \omega_i \text{ for all } i \text{ and } j. \tag{2.49}$$

Thus all we need to know is the ranking σ of ω_i, *i.e.*

$$\omega_{\sigma(0)} < \omega_{\sigma(1)} < ... < \omega_{\sigma(L-1)},$$

where σ gives the permutation of the indices that orders ω_i. As before, the negative threshold configuration can be written as,

$$z_i^- = \omega_i + \delta_{i,k^-}, \tag{2.50}$$

while the corresponding positive threshold configuration is given as,

$$z_i^+ = \omega_i + \delta_{i,\sigma(0)} + \delta_{i,\sigma(1)} - \delta_{i,k^+}, \tag{2.51}$$

where $\sigma(0)$ and $\sigma(1)$ are the lowest ranking sites. The site k^+ is determined by using

divisibility condition, Equation 2.31,

$$k^+ = \sigma(0) + \sigma(1) - k^-. \tag{2.52}$$

The ZFA changes the well numbers, m_i, in a way that the conditions on the Δm_i, Equation 2.30 and Equation 2.31, are always satisfied.

We can simplify our notation by labeling sites by their integer rank and using over and under bar to denote additions by ± 1. In this notation,

$$\begin{aligned} z_{\sigma(i)} &= \omega_{\sigma(i)} \leftrightarrow i \\ z_{\sigma(i)} &= \omega_{\sigma(i)} + 1 \leftrightarrow \overline{i} \\ z_{\sigma(i)} &= \omega_{\sigma(i)} - 1 \leftrightarrow \underline{i} \end{aligned}$$

Let us proceed with an example. Suppose the rank diagram of a negative threshold configuration is given by

$$4 \quad 2 \quad 13 \quad 0 \quad 3 \quad 9 \quad 12 \quad \overline{10} \quad 14 \quad 8 \quad 5 \quad 6 \quad 1 \quad 7 \quad 11. \tag{2.53}$$

Here our system consists of $L = 15$ sites and $k^- = \sigma(10)$.

With this notation, we can rewrite the ZFA as follows:

(i) Find the greatest integer that has a bar on it, let us say that this site has rank t.

(ii) Decrease this site's well coordinate by -2, this means that the site will acquire a negative defect,

$$\overline{t} \to \underline{t}. \tag{2.54}$$

(iii) Increase the well coordinates of its nearest neighbours by 1, meaning that if the neighbouring site has no defect, it will get a positive defect, and if it has negative

defect, the underbar will be removed,

$$\begin{aligned} \text{if it has no defect } \sigma(t) \pm 1 &\rightarrow \overline{\sigma(t) \pm 1}, \\ \text{if it has negative defect } \underline{\sigma(t) \pm 1} &\rightarrow \sigma(t) \pm 1. \end{aligned} \tag{2.55}$$

(iv) If any of the new coordinates have positive defect and have rank greater than t, go to step 2. Repeat this process until all particles that have a bar on it have smaller ranking than t.

2.1.4. Example: Threshold to Threshold Evolution

We will first investigate how a negative threshold configuration evolves into the positive threshold configuration, under the ZFA. To illustrate this let us again return to our previous example. Here

$$4 \quad 2 \quad 13 \quad 0 \quad 3 \quad 9 \quad 12 \quad \overline{10} \quad 14 \quad 8 \quad 5 \quad 6 \quad 1 \quad 7 \quad 11, \tag{2.56}$$

is the negative threshold configuration and

$$4 \quad 2 \quad 13 \quad \overline{0} \quad 3 \quad 9 \quad 12 \quad 10 \quad \underline{14} \quad 8 \quad 5 \quad 6 \quad \overline{1} \quad 7 \quad 11. \tag{2.57}$$

is the positive threshold configuration that we intende to reach under repeated applications of the ZFA.

Let us go through the first avalanche starting from the negative threshold configuration 2.56.

$$4 \quad 2 \quad 13 \quad 0 \quad 3 \quad 9 \quad 12 \quad \overline{10} \quad 14 \quad 8 \quad 5 \quad 6 \quad 1 \quad 7 \quad 11, \tag{2.58}$$

From the ZFA, the site an overbar and highest rank is 10. Therefore, the first avalanche

is triggered by the rank 10 site. From the step (ii) and (iii) of the ZFA,

$$\overline{10} \to \underline{10}, \tag{2.59}$$

$$12 \to \overline{12}, \tag{2.60}$$

$$14 \to \overline{14}. \tag{2.61}$$

Our configuration becomes

$$4 \quad 2 \quad 13 \quad 0 \quad 3 \quad 9 \quad \overline{12} \quad \underline{10} \quad \overline{14} \quad 8 \quad 5 \quad 6 \quad 1 \quad 7 \quad 11, \tag{2.62}$$

From the step (iv) of the ZFA for the rank diagram, the well coordinates of the rank 12 and 14 sites are greater than that of 10 so our first avalanche wave spreads further with 12 and 14 jumping as well, The effect of these jumps results in

$$\overline{12} \to \underline{12}, \tag{2.63}$$

$$\underline{10} \to 10, \tag{2.64}$$

$$9 \to \overline{9}. \tag{2.65}$$

$$\overline{14} \to \underline{14}, \tag{2.66}$$

$$10 \to \overline{10}, \tag{2.67}$$

$$8 \to \overline{8}. \tag{2.68}$$

and the new state becomes,

$$4 \quad 2 \quad 13 \quad 0 \quad 3 \quad \overline{9} \quad \underline{12} \quad \overline{10} \quad \underline{14} \quad \overline{8} \quad 5 \quad 6 \quad 1 \quad 7 \quad 11, \tag{2.69}$$

This first avalanche wave does not spread further because the sites ranked 9 and 8 does not jump. Therefore this is the first avalanche wave. Next, the rank 10 site jumps again, since it still has the largest well coordinate, $z_{\sigma(10)}$. From steps (ii) and (iii) of

the ZFA we find

$$\overline{10} \to \underline{10}, \tag{2.70}$$

$$\underline{12} \to 12, \tag{2.71}$$

$$\underline{14} \to 14 \tag{2.72}$$

and our state now becomes

$$4 \quad 2 \quad 13 \quad 0 \quad 3 \quad \overline{9} \quad 12 \quad \underline{10} \quad 14 \quad \overline{8} \quad 5 \quad 6 \quad 1 \quad 7 \quad 11. \tag{2.73}$$

In the first avalanche wave $12, 14$ and 10 jumped and in the second avalanche wave only 10 jumped. Note that the rank 10 will not jump again. The avalanche waves initiated at this site therefore terminate and the avalanche quiesces. The configuration 2.73 is a new configuration. In fact it can be readily shown [8] that the left and right extents of the avalanche waves decrease by one each time they are triggered. This sequence of waves terminates when the extent of one of the waves becomes zero. Thus in the avalanche example given, we started with an avalanche wave of left and right extent 1. The extents of the second wave were therefore each 0 and the the avalanche terminated after the second wave.

We do not need to work out all intermediate steps of the ZFA as in the previous example. We can determine the configuration reached after avalanche without having to resolve it into individual avalanche waves. An avalanche upon its first wave spreads as far to the left and right until it hits a negative defect site or a site that has a rank smaller than that of the initiating sites. Subsequent avalanche waves decrement theses initial left and right extents until one of the extends becomes zero. This allows us to resolve an avalanche process in a single step as follows [8]:

(i) Find the greatest integer that has a bar on it, suppose this is the site with rank t.

(ii) Find the left and right end of the avalanche, j_L and j_R respectively, where the j_L

is the first site on the left that has an underbar or rank smaller than t. Likewise, find j_R.

(iii) Then, update the following four sites,

- $\overline{t} \to t$,
- if j_L (j_R) has a under bar, $\underline{j_L} \to j_L$ ($\underline{j_R} \to j_R$),
- if j_L (j_R) has no defect, $j_L \to \overline{j_L}$ ($j_R \to \overline{j_R}$),
- $k \to \underline{k}$.

(iv) Where site k is calculated by divisibility condition, Equation 2.34,

$$k = j_L + j_R - t \pmod{L} \tag{2.74}$$

Proceeding with the evolution, the next avalanche is triggered by the rank 9 site and extends on the left and right to the rank 3 and 10 sites, respectively. Thus $j_L = j_R = 2$ The avalanche will therefore terminate after two avalanche waves and we reach the configuration:

$$4 \quad 2 \quad 13 \quad \overline{0} \quad 3 \quad \underline{9} \quad 12 \quad 10 \quad 14 \quad \overline{8} \quad 5 \quad 6 \quad 1 \quad 7 \quad 11. \tag{2.75}$$

The next avalanche is triggered by the rank 8 site with $j_L = 4$ and $j_R = 3$ and we reach the following configuration:

$$4 \quad 2 \quad 13 \quad \overline{0} \quad 3 \quad 9 \quad 12 \quad 10 \quad \underline{14} \quad 8 \quad 5 \quad 6 \quad \overline{1} \quad 7 \quad 11. \tag{2.76}$$

This is the positive threshold configuration 2.57. Let us see what happens if we applied the ZFA to this. The next avalanche would be triggered by the rank 1 site. Noting the periodic boundary conditions, the right and left extents both terminate at the rank 0 site. This means that the first avalanche wave will reach this site from both the left and right, and thus it will be forced to jump. As a result all sites have jumped

and the configuration is depinned.

2.1.5. ZFA Evolution and the Rank Representation for General S

The considerations so far applied to the case when $S = 1$, Equation 2.35. It turns out the case of general S is entirely analoguous, as we show now.

Let us define $\zeta_i \equiv \omega_i + J_i$ so that $\zeta_i \in \left(-\frac{1}{2} + a, \frac{1}{2} + a\right)$ where a is some real number that depends on J_i. The difference between the maximum and minimum elements of ζ_i is still less than 1. Let π therefore denote the permutation that orders the ζ_i,

$$\zeta_{\pi(0)} < \zeta_{\pi(1)} < ... < \zeta_{\pi(L-1)} \tag{2.77}$$

Then, any negative threshold configuration can be written as,

$$z_i^- = \zeta_i + \delta_{i,k_-}, \tag{2.78}$$

while the positive threshold configuration is given by

$$z_i^+ = \zeta_i - \delta_{i,k_+} + \delta_{i,\pi(0)} + \delta_{i,\pi(1)}. \tag{2.79}$$

Comparing with the corresponding threshold configurations, Equation 2.50 and Equation 2.51, we see that in terms of the rank representation, the ZFA proceeds as in the case of $S = 1$.

2.1.6. The Active Region

As we have seen in the $S = 1$ threshold to threshold evolution example, no avalanche can spread beyond the interval bounded by the rank 0 and 1 and containing

the site k^-. We will refer to the interior of this interval, *i.e.* excluding the rank 0 and 1 sites, as the active region. The sites outside of this interval are inactive, since none of these particles will jump, unless the configuration is depinned.

In our example of Subsection 2.1.4 the active region is

$$3 \quad 9 \quad 12 \quad \overline{10} \quad 14 \quad 8 \quad 5 \quad 6, \tag{2.80}$$

and we denote its lenght by ℓ, so that $\ell = 8$ for our example.

3. THE DISTRIBUTION OF THE NUMBER OF AVALANCHES IN THE THRESHOLD TO THRESHOLD EVOLUTION

Our aim in this Chapter is to the find the probability distribution for the number of avalanches in the threshold to threshold evolution, $P_L(N)$. In order to do so we will have to enumerate all possible configurations that will give rise to a given number of avalanches. Since the threshold to threshold evolution can be represented in terms of the rank diagram, this is equivalent to enumerating the number of permutations compatible with a given number of avalanches. Mungan and Kaspar have shown [8] that as a result of the statistical properties of the random phases α_i, these permutations are all equally likely. Thus a calculation of the distribution of the number of avalanches reduces to a count of compatible permutations π.

As we have seen in the previous Chapter, in the course of threshold to threshold evolution, only sites that are in the active region jump. We are only interested in these sites and the relative ranking of them. Let ℓ denote the length of the active region. If we return to the example of the previous Chapter, the negative and positive threshold configurations are,

$$4 \quad 2 \quad 13 \quad 0 \quad 3 \quad 9 \quad 12 \quad \overline{10} \quad 14 \quad 8 \quad 5 \quad 6 \quad 1 \quad 7 \quad 11, \tag{3.1}$$

$$4 \quad 2 \quad 13 \quad \overline{0} \quad 3 \quad 9 \quad 12 \quad 10 \quad \underline{14} \quad 8 \quad 5 \quad 6 \quad \overline{1} \quad 7 \quad 11. \tag{3.2}$$

As we have seen, the sites that jump in the course of the threshold to threshold evolution are,

$$3 \quad 9 \quad 12 \quad \overline{10} \quad 14 \quad 8 \quad 5 \quad 6. \tag{3.3}$$

$L = 15$ but $\ell = 8$. If we re-rank these sites, we obtain the following representation,

$$0 \quad 4 \quad 6 \quad \overline{5} \quad 7 \quad 3 \quad 1 \quad 2. \tag{3.4}$$

Thus configurations 3.1, 3.3 and 3.4 are three equivalent representation as far as evolution in the subthreshold regime is concerned.

We know the probability distribution of ℓ for given L,

$$P(\ell|L) = \begin{cases} \dfrac{2}{L(L-1)}\ell & \text{if } 1 \leq \ell \leq L-2 \\ \dfrac{2}{L} & \text{if } \ell = 0. \end{cases} \tag{3.5}$$

Therefore if we can find $P(N|\ell)$ for each ℓ, we can determine the $P_L(N)$,

$$P_L(N) = \sum_{\ell=0}^{L-2} p_L(\ell) P(N|\ell). \tag{3.6}$$

For a given ℓ, there are $\ell! \times \ell$ different negative threshold configurations. The $\ell!$ term comes from the different permutations of sites and the ℓ factor comes from the different places where to put an overbar. All these different configurations contribute equally to $P_L(N)$.

When we look at the threshold to threshold evolution of any configuration, we can easily see that avalanches terminate at the sites that have smaller rank than $\pi(k^-)$. Therefore, the number of avalanches in the evolution depends only on the relative location of the site $\pi(k^-)$ and the location of the sites that have rank smaller than $\pi(k^-)$. These sites are the records of the $\zeta_i, i \in [i_L, i_R]$. The connection between our threshold to threshold evolution and the records statistics is explained in the Appendix.

We can simplify our calculation further by partitioning the possible configurations into groups that have different $\pi(k^-)$. We have ℓ groups because $\pi(k^-)$ can take values

$\{0, 1, ..., \ell - 1\}$ and the contribution from all $\pi(k^-)$ is equal. Write,

$$P(N|\ell) = \sum_{\pi(k^-)=0}^{\ell-1} P(\pi(k^-)|\ell) P(N|\pi(k^-), \ell), \tag{3.7}$$

where $P(\pi(k^-)|\ell) = \frac{1}{\ell}$.

Also note that for given $\pi(k^-)$, the $P(N|\pi(k^-), \ell)$ is independent of ℓ, and it only depends on the relative distribution of the sites $\{\pi(0), \pi(1), ..., \pi(k^-)\}$, because any site that has a greater rank than the avalanche trigger site cannot be a avalanche initiator k^-. All avalanche triggers, except the first one, $\pi(k^-)$, are the termination sites of one of the earlier avalanches and any avalanche in the threshold to threshold evolution ends with site that has smaller rank. Therefore,

$$P(N|\pi(k^-), \ell) = P(N|\pi(k^-)). \tag{3.8}$$

Let us return to our example. We have already shown that the following two configurations are equivalent when we look at the number of avalanches in the threshold to threshold evolution.

$$4 \quad 2 \quad 13 \quad 0 \quad 3 \quad 9 \quad 12 \quad \overline{10} \quad 14 \quad 8 \quad 5 \quad 6 \quad 1 \quad 7 \quad 11, \tag{3.9}$$

$$0 \quad 4 \quad 6 \quad \overline{5} \quad 7 \quad 3 \quad 1 \quad 2. \tag{3.10}$$

We now show that these configurations are also equivalent to a *reduced configuration*, as far as the number of avalanches are conserved. The reduced configuration is the configuration that only contains sites in the active region that have rank equal or smaller than $\pi(k^-)$.

$$0 \quad 4 \quad \overline{5} \quad 3 \quad 1 \quad 2. \tag{3.11}$$

Let us next introduce the *level, i*, which is the location of $\pi(k^-)$ in the reduced configuration. In our example *level* $i = 3$. For any reduced configuration we have: $1 < i < \pi(k^-) + 1$. We can also show that for given $\pi(k^-)$, the contribution from all the *levels* is equal so that $P(i|\pi(k^-)) = \frac{1}{\pi(k^-)+1}$. We can therefore write,

$$P(N|\pi(k^-)) = \sum_{i=0}^{\pi(k^-)+1} P(i|\pi(k^-))P(N|i,\pi(k^-)). \tag{3.12}$$

We next obtain the probability distribution for the number of avalanches in the threshold to threshold evolution, for given $\pi(k^-)$ and i, which we donote by $P(N|i,\pi(k^-))$.

$$P_L(N) = \sum_{\ell=0}^{L-2} p_L(\ell) \sum_{\pi(k^-)=0}^{\ell-1} P(\pi(k^-)|\ell) \left[\sum_{i=1}^{\pi(k^-)+1} P(i|\pi(k^-))P(N|i,\pi(k^-)) \right]. \tag{3.13}$$

3.1. Determining $P(N|i,\pi(k^-))$

We will determine $P(N|i,\pi(k^-))$ for any *level* i, recursively starting with $i = 1$. Any configurations that has *level 1* has the following structure,

$$\overline{\pi(k^-)} \quad a_1 \quad a_2 \quad a_3 \quad ... \quad a_{\pi(k^-)}, \tag{3.14}$$

where $a_j = 0, 1, 2, ..., \pi(k^-) - 1$, for $\pi(k^-) \geq j \geq 1$. We show that the number of avalanches in the threshold to threshold evolution depends only on the location of sites that have rank smaller than $\pi(k^-)$.

After the first avalanche our configuration becomes;

$$\underline{\pi(k^-)} \quad \overline{a_1} \quad a_2 \quad a_3 \quad ... \quad a_{\pi(k^-)} \tag{3.15}$$

As we mentioned above, the location of the negative defect does not change the total number of avalanches in the threshold to threshold evolution, so we can use this notation without loss of generality.

If we look at the last configuration, we can see that our system will have all further avalanches to the right. After the first avalanche wave a_1 definitely gets an overbar, because it is smaller than $\pi(k^-)$ and there is no site between $\pi(k^-)$ and a_1 that has smaller rank than $\pi(k^-)$. So our first avalanche should be terminated at the site a_1. The above configuration acts as a level one configuration that has $\pi'(k^-) = a_1$ where $a_1 \in \{0, 1, 2, ..., (\pi(k^-) - 1)\}$. Again, a_1 can have all these values with equal probability.

As we explain in the Appendix, the probability of having k records in the sequence of n numbers is given by Equation A.8. In the Appendix we also show that in the reduced negative threshold configuration the threshold to threshold evolution after the first avalanche is goverened by a record process. So $\pi(k_-)$ sites remain available for $N - 1$ records, so that including the last one there is total N records, *i.e.* avalanches.

Thus, the probability of having N avalanches for a level one configuration is given as

$$P(N|i = 1, \pi(k^-)) = \frac{1}{\pi(k^-)!} \begin{bmatrix} \pi(k^-) \\ N - 1 \end{bmatrix}. \tag{3.16}$$

This result is important, because we will be able to write the probability distribution of avalanches for any other *level* in terms of this.

The *level i* configuration can be written as,

$$a_1 \quad a_2 \quad a_3 \quad ... \quad a_{i-1} \quad \overline{\pi(k^-)} \quad a_i \quad ... \quad a_{\pi(k^-)}. \tag{3.17}$$

After the first avalanche our configuration becomes;

$$a_1 \quad a_2 \quad a_3 \quad ... \quad \overline{a_{i-1}} \quad \underline{a_{\pi(k^-)}} \quad \overline{a_i} \quad ... \quad a_{\pi(k^-)} \tag{3.18}$$

As we discussed in the Appendix, after the first avalanche our system acts as two independent level one systems. The subsystem that is on the left is,

$$a_1 \quad a_2 \quad a_3 \quad ... \quad a_{i-1} \quad \overline{a_{\pi(k^-)}} \tag{3.19}$$

while the subsystem that is on the right is,

$$\overline{a_{\pi(k^-)}} \quad a_i \quad ... \quad a_{\pi(k^-)}. \tag{3.20}$$

When we re-rank these two configuration as two separate configuration, the first one is a level 1 system that has $\pi'(k^-) = i - 1$. The second subsystem will have $\pi''(k^-) = \pi(k^-) - i + 1$ and again level one. However, their first avalanche is common. Therefore, when the first subsystem has s avalanches, the second system must have $N - (s - 1)$ in order for our total system to have N avalanches. We can hence write the probability distribution of avalanches for any *level* as

$$P(N|i, \pi(k^-)) = \sum_{s=1}^{N} \frac{1}{(i-1)!} \begin{bmatrix} i-1 \\ s-1 \end{bmatrix} \frac{1}{(\pi(k^-) - i + 1)!} \begin{bmatrix} \pi(k^-) - i + 1 \\ N - s \end{bmatrix}, \tag{3.21}$$

where the sum is over all possible s values. In this equation $\frac{1}{(i-1)!} \begin{bmatrix} i-1 \\ s-1 \end{bmatrix}$ is the probability distribution of having s avalanches in the left direction and the $\frac{1}{(\pi(k^-) - i + 1)!} \begin{bmatrix} \pi(k^-) - i + 1 \\ N - s \end{bmatrix}$ term is the probability of having $N - (s - 1)$ avalanches in the right direction. Together with the common first avalanche the total number of avalanches is N.

3.2. Determining $P_L(N)$

For given $\pi(k^-)$ and *level*, we have found the probability for the number of avalanches in the threshold to threshold evolution. Therefore when we substitute this result, Equation 3.21, into into Equation 3.13 find:

$$P_L(N) = \sum_{\ell=0}^{L-2} p_L(\ell) \sum_{\pi(k^-)=0}^{\ell-1} P(\pi(k^-)|\ell) \times \left[\sum_{i=1}^{\pi(k^-)+1} P(i|\pi(k^-)) \sum_{s=1}^{N} \frac{1}{(i-1)!} \begin{bmatrix} i-1 \\ s-1 \end{bmatrix} \frac{1}{(\pi(k^-)-i+1)!} \begin{bmatrix} \pi(k^-)-i+1 \\ N-s \end{bmatrix}, \right]. \quad (3.22)$$

Let us substitute the probabilities so that Equation 3.22 becomes,

$$P_L(N) = \sum_{\ell=1}^{L-2} \left(\frac{2\ell}{L(L-1)} \right) \sum_{\pi(k^-)=0}^{\ell-1} \frac{1}{\ell} \sum_{i=1}^{\pi(k^-)+1} \frac{1}{\pi(k^-)+1} \times \left[\sum_{s=1}^{N} \frac{1}{(i-1)!} \begin{bmatrix} i-1 \\ s-1 \end{bmatrix} \frac{1}{(\pi(k^-)-i+1)!} \begin{bmatrix} \pi(k^-)-i+1 \\ N-s \end{bmatrix}, \right] + \frac{2}{L}\delta_{N,0}. \quad (3.23)$$

In order to simplify this further let us make the following change of variables:

$$\ell \to k,$$
$$\pi(k^-) \to j-1.$$

Exchanging the order of the i sum, Equation 3.23 becomes,

$$P_L(N) = \sum_{k=1}^{L-2} \left(\frac{2}{L(L-1)} \right) \sum_{j=1}^{k} \frac{1}{j} \sum_{s=1}^{N} \times \left[\sum_{i=1}^{j} \frac{1}{(i-1)!} \begin{bmatrix} i-1 \\ s-1 \end{bmatrix} \frac{1}{(j-i)!} \begin{bmatrix} j-i \\ N-s \end{bmatrix}, \right] + \frac{2}{L}\delta_{N,0}. \quad (3.24)$$

Equation 3.24 by itself is not very useful for computational calculations or in

order to understand this result. Therefore, we should simplify Equation 3.24 further.

Using the Equation A.15 given in the Appendix, we can write,

$$\sum_{i=1}^{j} \frac{1}{(i-1)!} \begin{bmatrix} i-1 \\ s-1 \end{bmatrix} \frac{1}{(j-i)!} \begin{bmatrix} j-i \\ N-s \end{bmatrix} = \frac{1}{(j-1)!} \begin{bmatrix} j-1 \\ N-1 \end{bmatrix} \binom{N-1}{s-1}. \tag{3.25}$$

So Equation 3.24 becomes,

$$P_L(N) = \sum_{k=1}^{L-2} \left(\frac{2}{L(L-1)} \right) \sum_{j=1}^{k} \frac{1}{j} \sum_{s=1}^{N} \left[\frac{1}{(j-1)!} \begin{bmatrix} j-1 \\ N-1 \end{bmatrix} \binom{N-1}{s-1} \right] + \frac{2}{L} \delta_{N,0}. \tag{3.26}$$

This can be rearranged as

$$P_L(N) = \frac{2}{L(L-1)} \sum_{k=1}^{L-2} \sum_{j=1}^{k} \frac{1}{j} \frac{1}{(j-1)!} \begin{bmatrix} j-1 \\ N-1 \end{bmatrix} \sum_{s} \binom{N-1}{s-1} + \frac{2}{L} \delta_{N,0}. \tag{3.27}$$

Here the binomial coefficient sum is over all none-zero terms and thus will give us,

$$\sum_{s} \binom{N-1}{s-1} = 2^{N-1}. \tag{3.28}$$

Equation 3.27 then becomes,

$$P_L(N) = \frac{2^N}{L(L-1)} \sum_{k=1}^{L-2} \sum_{j=1}^{k} \frac{1}{j!} \begin{bmatrix} j-1 \\ N-1 \end{bmatrix} + \frac{2}{L} \delta_{N,0}. \tag{3.29}$$

Now, let us exchange the order of the two sums so all variables are independent of k and thus

$$P_L(N) = \frac{2^N}{L(L-1)} \sum_{j=1}^{L-2} \frac{1}{j!} \begin{bmatrix} j-1 \\ N-1 \end{bmatrix} \sum_{k=j}^{L-2} + \frac{2}{L} \delta_{N,0}, \tag{3.30}$$

Figure 3.1. Lines correspond to Equation 3.32 for five different system size L. The dots give the distribution of the total number of steps in the threshold to threshold evolution obtained from numerical simulations. The number of realizations is given in parentheses next to their corresponding L.

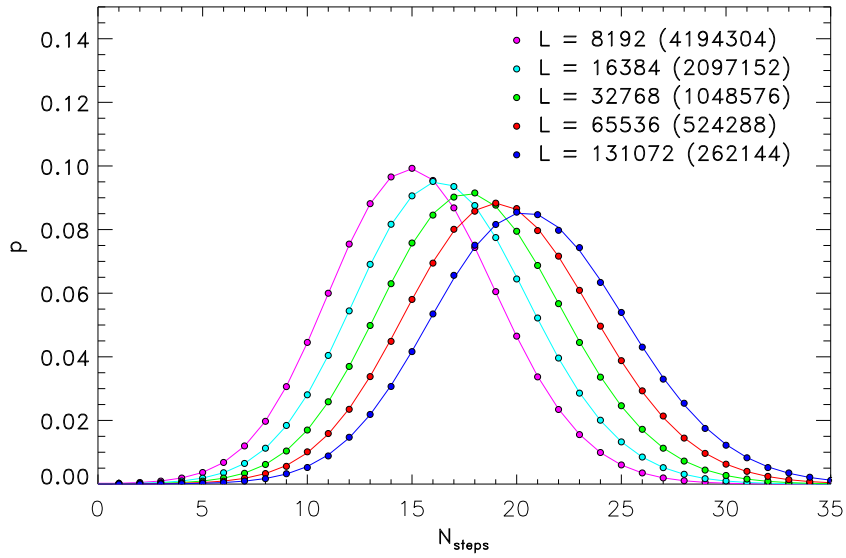

Finally doing the sum over k,

$$P_L(N) = \frac{2^N}{L(L-1)} \sum_{j=1}^{L-2} \frac{(L-j-1)}{j!} \begin{bmatrix} j-1 \\ N-1 \end{bmatrix} + \frac{2}{L}\delta_{N,0}. \tag{3.31}$$

This result can be simplified further and after the simplification we end up with the following equation

$$P_L(N) = \frac{2^N}{L!} \sum_{t=N+1}^{L-1} \begin{bmatrix} L-1 \\ t \end{bmatrix} + \frac{1}{L}\delta_{N,0}. \tag{3.32}$$

Intermediate steps can be found in the Appendix.

3.2.1. Comparison with Numerical results

Equation 3.32 gives the exact probability distribution of steps in the threshold to threshold evolution. Figure 3.1 shows that our result fit perfectly to results that we obtain from numerical simulations.

3.2.2. Determining $\mathbb{E}N$

$\mathbb{E}N$ can be calculated by using the generating function for $P_L(N)$. Let us write down the generating function.

$$g(z) = \sum_{N=0}^{L-2} z^N \frac{2^N}{L!} \sum_{t=N+1}^{L-1} \begin{bmatrix} L-1 \\ t \end{bmatrix} + \frac{1}{L}. \tag{3.33}$$

Moving t sum to the left and changing the place of the two sums,

$$g(z) = \sum_{t=1}^{L-2} \sum_{N=0}^{t-1} \frac{(2z)^N}{L!} \begin{bmatrix} L-1 \\ t \end{bmatrix} + \frac{1}{L}. \tag{3.34}$$

If we do the sum over N,

$$g(z) = \frac{1}{L!} \sum_{t=1}^{L-2} \frac{1-(2z)^t}{1-2z} \begin{bmatrix} L-1 \\ t \end{bmatrix} + \frac{1}{L}. \tag{3.35}$$

Equation 3.35 can be written as

$$g(z) = \frac{1}{(1-2z)L!} \sum_{t=1}^{L-1} \begin{bmatrix} L-1 \\ t \end{bmatrix} - \frac{1}{(1-2z)L!} \sum_{t=1}^{L-1} (2z)^t \begin{bmatrix} L-1 \\ t \end{bmatrix} + \frac{1}{L}. \tag{3.36}$$

Using the identities Equation A.16 and Equation A.17 for the first and the second term in Equation 3.36, respectively,

$$g(z) = \frac{1}{(1-2z)L} - \frac{1}{(1-2z)L!}\{2z(2z+1)(2z+2)...(2z+L-2)\} + \frac{1}{L}. \tag{3.37}$$

From the normalization condition on the probability distribution $P_L(N)$, Equation 3.37 must satisfy $g(1) = 1$. Indeed,

$$g(1) = \frac{1}{(1-2)L} - \frac{1}{(1-2)L!}\{2(2+1)...(2+L-2)\} + \frac{1}{L} = -\frac{1}{L} + \frac{L!}{L!} + \frac{1}{L} = 1. \tag{3.38}$$

The mean value of the number of avalanches in the threshold to threshold evolution is given by,

$$\mathbb{E}N = \left.\frac{\partial g(z)}{\partial z}\right|_{z=1}. \tag{3.39}$$

If we take the derivative of Equation 3.37 with respect to z,

$$\begin{aligned}\frac{\partial g(z)}{\partial z} = \frac{2}{(1-2z)^2 L} - \frac{2}{(1-2z)^2 L!}\{2z(2z+1)(2z+2)...(2z+L-2)\} \\ - \frac{1}{(1-2z)L!}[\{2(2z+1)(2z+2)...(2z+L-2)\} \\ + \{2z(2)(2z+2)...(2z+L-2)\} + \{2z(2z+1)(2)(2z+3)...(2z+L-2)\} \\ + ...\{2z(2z+1)(2z+2)...(2z+L-3)(2)\}].\end{aligned} \tag{3.40}$$

The third term in Equation 3.40 can be written as a sum,

$$\begin{aligned}\frac{\partial g(z)}{\partial z} = \frac{2}{(1-2z)^2 L} - \frac{2}{(1-2z)^2 L!}\{2z(2z+1)(2z+2)...(2z+L-2)\} \\ - \frac{2}{(1-2z)L!}\sum_{j=2z}^{j=2z+L-2}\frac{2z(2z+1)(2z+2)...(2z+L-2)}{j}.\end{aligned} \tag{3.41}$$

Let us calculate Equation 3.41 at $z = 1$,

$$\left.\frac{\partial g(z)}{\partial z}\right|_{z=1} = \frac{2}{L} - 2 + \frac{2}{L!}\sum_{j=2}^{j=L}\frac{L!}{j}. \tag{3.42}$$

Therefore, the mean value of the number of avalanches in the threshold to threshold evolution becomes,

$$\mathbb{E}N = 2\left(1 + \sum_{j=2}^{j=L}\frac{1}{j}\right) - 4 + \frac{2}{L}, = 2\sum_{j=1}^{j=L}\frac{1}{j} - 4 + \frac{2}{L}. \tag{3.43}$$

It can be written as

$$\mathbb{E}N = 2H_L - 4 + \frac{2}{L}, \tag{3.44}$$

where $H_L = \sum_{j=1}^{L} \frac{1}{j}$ is a harmonic number.

4. HYSTERESIS BEHAVIOUR

As we discussed in the second Chapter, our system exhibits irreversible behaviour. This irreversible behaviour occurs if the external force F is increased decreased such that this causes a jump of one or more particles. As Kaspar and Mungan have shown, when the applied force is returned back to zero none of the particles jump. Actually this behaviour enables us to use the equivalent configurations with zero force (ZF), $F = O$.

4.1. Force Cycles and Hysteresis Loops

We can ask what happens when we start with a configuration, change the force in one direction until one or more avalanches occurs, then change the force in the opposited direction until again particles jump and finally return the force to its initial value. We will call such a sequence of force increments and decrements a force cycle. In general, under a force cycle a static configuration will not to its original form, even though the force has been brought back to its original value.

In terms of the equivalent ZFA configurations, the action of a force cycle is as follows. We apply the ZFA, one or more times in one direction, making sure that the configurations remain stable and then reverse the direcion of the ZFA.

To illustrate this, consider the following configuration

$$4 \quad 2 \quad 13 \quad 0 \quad 3 \quad 9 \quad 12 \quad \overline{10} \quad 14 \quad 8 \quad 5 \quad 6 \quad 1 \quad 7 \quad 11,$$

apply the ZFA in the positive in the positive direction,

(i) Find the greatest integer that has a bar on it is 10,

(ii) The left end of the avalanche is $i_L = 9$ and the right end of the avalanche is $i_R = 8$,

(iii) Make the following jumps

- $\overline{10} \to 10$,
- $9 \to \overline{9}$ and $8 \to \overline{8}$,
- $10 \to \underline{10}$.

Our configuration becomes,

$$4 \quad 2 \quad 13 \quad 0 \quad 3 \quad \overline{9} \quad 12 \quad \underline{10} \quad 14 \quad \overline{8} \quad 5 \quad 6 \quad 1 \quad 7 \quad 11. \tag{4.1}$$

When we next apply the ZFA once in the negative direction, it causes the following changes,

- $\underline{10} \to 10$,
- $12 \to \underline{12}$ and $14 \to \underline{14}$,
- $10 \to \overline{10}$.

Then our system transits into

$$4 \quad 2 \quad 13 \quad 0 \quad 3 \quad \overline{9} \quad \underline{12} \quad \overline{10} \quad \underline{14} \quad \overline{8} \quad 5 \quad 6 \quad 1 \quad 7 \quad 11. \tag{4.2}$$

Comparing configuration 4.1 with the above configuration, we see that our system does not return to its initial configuration.

By application of force cycles we can construct a hysteresis loops. In hysteresis loops, under the application of an appropriate force cycle, we strat from one configuration, transit into another one by a sequence of avalanches in one direction and then come back to the initial configuration by another sequence of avalanches in the opposite direction.

There are two special configurations that allow us to construct such a loop. These

are the threshold configurations, since we know that every configuration transits into a threshold configuration by a finite number of avalanches in either one of the two possible directions.

Let us give an example of a hysteresis loop that contains both the negative and the positive threshold configuration. Consider a negative threshold configuration with an active region given by

$$5 \quad \overline{1} \quad 6 \quad 2 \quad 3 \quad 0 \quad 4 \quad 7 \tag{4.3}$$

If the ZFA is applied first in the positive direction, the configuration 4.3 transits into

$$5 \quad 1 \quad 6 \quad \underline{2} \quad 3 \quad \overline{0} \quad 4 \quad 7 \tag{4.4}$$

After applying the ZFA once more in the positive direction, the following configuration is found:

$$5 \quad 1 \quad 6 \quad 2 \quad 3 \quad 0 \quad \underline{4} \quad 7 \tag{4.5}$$

This is the positive threshold configuration. Let us next repeatedly apply the ZFA in the negative direction until we reach the negative threshold configuration:

$$5 \quad 1 \quad \underline{6} \quad \overline{2} \quad 3 \quad 0 \quad 4 \quad \underline{7} \tag{4.6}$$

$$\overline{5} \quad 1 \quad 6 \quad 2 \quad 3 \quad 0 \quad 4 \quad \underline{7} \tag{4.7}$$

$$5 \quad \overline{1} \quad 6 \quad 2 \quad 3 \quad 0 \quad 4 \quad 7 \tag{4.8}$$

The evolutions of states constituting the hysteresis loop is shown schematically in

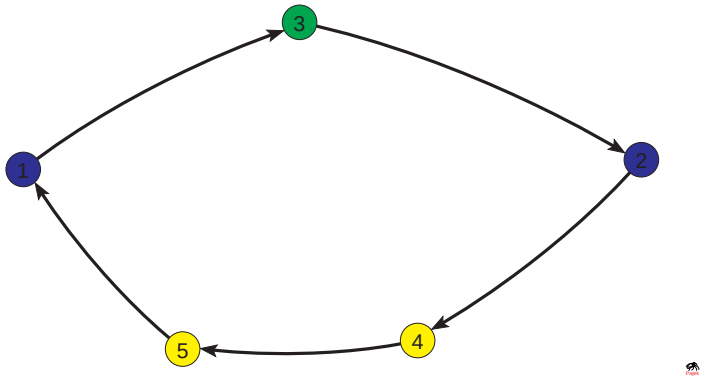

Figure 4.1. The representation of the hysteresis loop that contains the negative and the positive threshold configurations. In the figure every circle represents a distinct state such that $1, 2, 3, 4$ and 5 represents the configurations 4.3, 4.5, 4.4, 4.6 and 4.7, respectively. The black and the red arrows represent transitions.

Figure 4.1.

4.2. The Reachable states

The *reachable states* are the set of all states that can be reached from either of the two threshold configurations by a sequence of increasing and decreasing forces. We are interested in the relation between the system size L and the total number of reachable states. In order to obtain this relations, we have performed numerical simulations.

Each configuration can transits into two different *static* configurations: by either increasing the force or decrease it. The only exceptions are the positive and negative threshold configurations, that can transit only into a single static configuration, by a decrease or increase of the driving force, resepctively. A negative (positive) threshold configuration can not transits into a static configuration via force decrease (increase) because when the ZFA is applied to a negative (positive) threshold configuration in the negative (positive) direction our system depins and starts to slide.

4.3. Description of the Numerical Algorithm

We next describe the numerical algorithm that we used to list all reachable states, for a given system size L and realization of random phases α_i. We use the ZFA is used in order to transits between static configurations and maintain a pointer vector. The pointer vector contains all information about the connections between reachable configurations. Initially, the pointer vector contains only the negative and positive threshold configurations because they can be found directly, from the phases α_i, as shown before.

Let us illustrate this algorithm, on the example of the previous section, (the negative threshold configuration 4.3) to find all reachable states. The initial state of the pointer vector is given Table 4.1. We put the negative threshold configuration in the first row and the positive threshold configuration in the second row. The first column of each row specifies a unique ID for the corresponding configuration. The second and the third row specify the configuration we reach when we apply the ZFA in the positive and negative directions, respectively. **X** represents the forbidden transitions which are those into the sliding state. Only the threshold configurations have forbidden transitions because these two configuration are essentially unique, and thus the system can transit into the dynamic regime only from these two configurations. **?** represents the transitions that have not been determined yet. The aim of our algorithm is o resolve all transitions, while keeping track whether the states reached in this way have already occured or are new.

We start from one of the **?** and resolve it by applying the ZFA. If we transit into a configuration such that our pointer vector does not contain it, we add this configuration as a new row and put ?s to in the second and third colums.

Once we have resolved all ?, we have obtained all reachable states along with their connections. We can represent the pointer vector as a reachability graph.

In Table 4.1 every row corresponds to a different configuration. The first column

Table 4.1. This is the initial state of our pointer vector.

1	?	X	5	$\overline{1}$	6	2	3	0	4	7
2	X	?	5	1	6	2	3	0	$\underline{4}$	7

Table 4.2. This table shows the final state of our algorithm. It contains all reachable states and the transitions between them.

1	3	X	5	$\overline{1}$	6	2	3	0	4	7
2	X	4	5	1	6	2	3	0	$\underline{4}$	7
3	2	6	5	1	6	$\underline{2}$	3	$\overline{0}$	4	7
4	7	5	5	1	$\underline{6}$	$\overline{2}$	3	0	4	$\underline{7}$
5	8	1	$\overline{5}$	1	6	2	3	0	4	$\underline{7}$
6	3	9	5	1	$\underline{6}$	$\overline{2}$	$\underline{3}$	$\overline{0}$	4	7
7	2	4	5	1	6	2	$\underline{3}$	$\overline{0}$	4	$\underline{7}$
8	7	5	$\underline{5}$	$\overline{1}$	6	2	3	0	4	$\underline{7}$
9	6	1	5	1	$\underline{6}$	2	$\overline{3}$	0	4	7

provides a unique id for the configuration *i.e.* $1, 2, 3, 4...$, while the second and third columns specify the ids of the configurations we reach when we apply the ZFA in the positive and negative direction. The last column is a rank-diagram representation of the configuration. A ? means that we have not yet determined the outcome of the corresponding transition. An X indicates that the transition is forbidden.

Table 4.2 shows the pointer table after all reachable states and the transitions between them have been identified. Note that as a result, it does not contain any **?** anymore.

Using Table 4.2 we can draw the the reachability graph, Figure 4.2.

4.4. Numerical Results

We apply the algorithm outlined in the previous section, for various system sizes $L = 16, 32, 64, 128, 256$ using more than 10000 realizations of random phases. Plotting the the total number of reachable state averaged over the realizations, against

Figure 4.2. The reachability graph of our example showing all reachable states and the transitions between them. The red (black) arrows indicate transitions under applying the ZFA once in the positive (negative) direction.

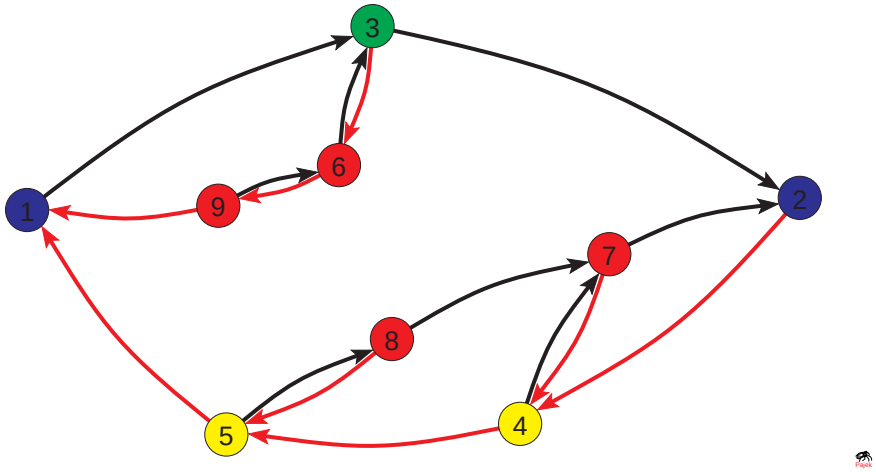

the system size, we find power law behaviour with an exponent of 3/2, as shown in Figure 4.4.

Every static configuration that satisfies the integer Equation 2.30 and divisibility Equation 2.31 conditions on Δm_i is a static condition. As a result the number of configurations satisfying these conditions increases exponentially with the system size. From the power law relation that we obtain, we conclude that only a small fractionof these static configurations are reachable states, *i.e.* states that can be reached from th the positive or negative threshold configuration by a sequence of force increments and decrements.

Let us next give an example of a reachability graph for a bigger system. Figure 4.4 shows the reachability graph for a system system of size $L = 32$.

From the Figure 4.4 it can be seen that there are hysteresis loops emebedded into larger loops. Some of these subloops acts as a reachability graph of a smaller system. For example the configurations 6 and 24 act as a threshold configuration for this subloop, since every configuration between 6 and 24 must transit into 6 or 24 before going to any state outside of this loop. We can see that there are many sub

Figure 4.3. Numerically obtained relation between the system size and the average of the total number of reachable states on a log-log scale (blue data points). The red line is a power-law with exponent 3/2.

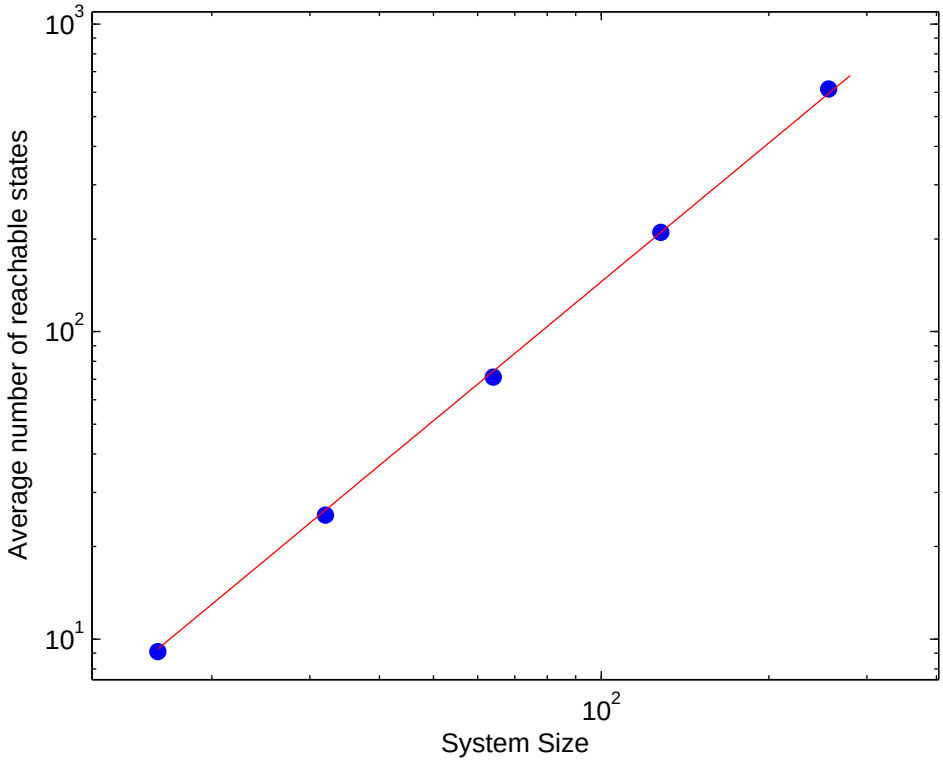

loops that have this property. Thus there is a hierarchy between reachable states in embedded loops.

4.4.1. Partial Ordering and Hierarchies

Kaspar and Mungan, [8], have shown that the toy model obey the no-passing rule of Middleton and Fisher [1]. This rule states that if for each site the well number of one configuration is greater or equal to the well numbers of the other configuration, and moreover the maximum of the well coordinate of the first configuration is greater than the maximum well coordinate of the second configuration, then the second configuration can not cross the first one as a result of avalanches in the positive direction.

The existence of hysteresis loops implies that the toy model exhibits the return-

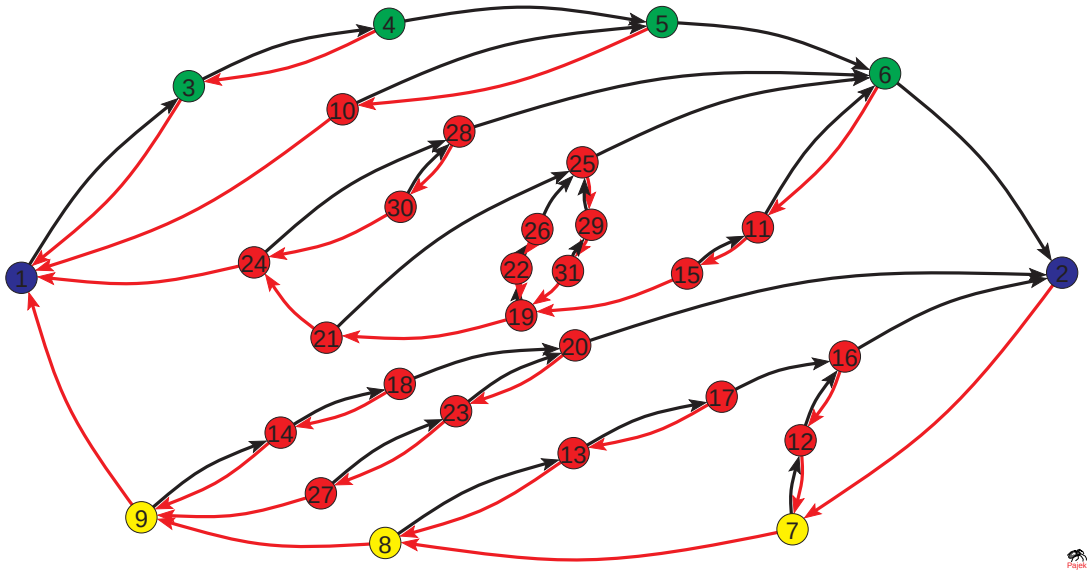

Figure 4.4. The reachability graph for a system of size $L = 32$.

point memory effect described by Sethna *et al.* [2]. Sethna *et al.* have shown that if the set of reachable configurations has partial ordering, the transitions obey the no-passing rule and the system is driven adiabatically, the return point memory effect will occur. This is rather remarkable, since the jumps of the particles release energy and thus the response of our system to force avalanches is not adiabatic, while on the other hand the toy model does exhibit partial ordering of reachable states and the no-passin rule. Thus the requirement of adiabaticity while sufficient does not seem to be necessary for return point memory.

5. CONCLUSION

We have investigated the properties of a simple charge density wave system in the subthreshold regime focusing on a toy model that was introduced by Kaspar and Mungan [8].

We determined analytically the probability distribution of the number of steps between the two threshold configurations. We obtained this result by noting that every configuration can be represented by a rank diagram. In particular, each configuration is determeined by a set of integers and distribution of bars. As we have seen, only a subset of sites is active in the static regime. Moreover, it turned out that only sites that have ranking greater or equal to sites $\pi(k^-)$ play a role in determining the intermediate configuration for the evolution from the negative to positive threshold. We used these observations to enumerate the configurations and thus the number of avalanches. As was shown by Kaspar and Mungan, the threshold to threshold evolution is governed by a record-breaking process. The probability distribution of the number of record is related to the Stirling numbers of the first kind. This allowed us to determine the probability distribution of the number of avalanches in the threshold to threshold evolution. We also checked our analytical result against numerical simulations and found excellent aggreement.

We then investigated the hysteretic behaviour of the toy model and found a hierarchical structure among reachable static configurations. We devised a numerical algorithm to enumerate all reachable states and used this to determine the relation between the system size L and the total number of reachable states. The number of all metastable states is expected to increasese exponentially with the system size. However, we observed a power law relation between the total number of reachable states and the system size and found an exponent 3/2. This result shows that one cannot reach all static configuration starting from the threshold configurations. Instead, we can only transit into a small part of all static configurations.

APPENDIX A: RECORD STATISTICS AND STIRLING NUMBERS

As Kaspar and Mungan [8] showed, the number of avalanches in the threshold to threshold evolution can be thought as a record process. This is a consequence of the fact that the avalanches are terminated at sites that have smaller rank than the trigger site of the avalanche. Therefore, as the system evolves from the negative to the positive threshold, it seeks to lower the records until it hits the lowest two sites, $\pi(0)$ and $\pi(1)$, to the left and the right.

Every negative threshold configuration can be written as a distribution of integers which represent the ranking of coordinates of sites and a overbar which represents the positive defect on the site $\pi(k^-)$. We also showed that in the threshold to threshold evolution only sites that have ranking $\pi(k^-)$ or smaller than $\pi(k^-)$ are important. When we increase the force starting from the negative threshold configuration, we observe two distinct record processes. Thes two record processes start from the site $\pi(k_-)$ and proceed to its left and right.

Let us consider the example in Chapter 2 again. The negative threshold configuration is,

$$4 \quad 2 \quad 13 \quad 0 \quad 3 \quad 9 \quad 12 \quad \overline{10} \quad 14 \quad 8 \quad 5 \quad 6 \quad 1 \quad 7 \quad 11, \tag{A.1}$$

and we showed that the following configuration is equivalent to configuration A.1 in the sense of the evolution from the negative to positive threshold configuration. The reduced configuration of configuration A.1

$$0 \quad 4 \quad \overline{5} \quad 3 \quad 1 \quad 2. \tag{A.2}$$

After the first avalanche in the positive direction, our system transits into the config-

uration

$$0 \quad \overline{4} \quad \underline{5} \quad \overline{3} \quad 1 \quad 2. \tag{A.3}$$

where the first avalanche terminated at the sites ranked 4 and 3. In this process, the places of negative defects do not change the number of avalanches in the threshold to threshold evolution so we can put an underbar on 5. We only need to keep track of the sites that have equal or smaller rank than site $\pi(k^-)$, because the avalanche waves in the evolution from negative to positive threshold configurations can only be terminated at these sites. Also, as we mentioned previously, in the reduced configuration the first avalanche must be terminated at nearest neighbours of site $\pi(k^-)$. Let us keep applying force in the positive direction. After the second avalanche our system transits into

$$\overline{0} \quad \underline{4} \quad 5 \quad \overline{3} \quad 1 \quad 2. \tag{A.4}$$

If we apply the ZFA to this configuration A.4, it next transits into

$$\overline{0} \quad 4 \quad \underline{5} \quad 3 \quad \overline{1} \quad 2. \tag{A.5}$$

After the fourth avalanche, the record process for the right part terminates.

$$\overline{0} \quad 4 \quad 5 \quad 3 \quad \underline{1} \quad 2. \tag{A.6}$$

Finally, with the last avalanche the record process for the left part also terminates and the system has reached the positive threshold configuration,

$$0 \quad 4 \quad 5 \quad \underline{3} \quad 1 \quad 2. \tag{A.7}$$

As one can see from this example we have two separate record processes. One of them is in the left of site $\pi(k^-)$ and the other one is to its right. These two record

processes are independent.

The probability of having k records in a sequence of n exchangeable random variables is given by [9],

$$P_{\text{records}}(k|n) = \frac{1}{n!}\begin{bmatrix} n \\ k \end{bmatrix}. \tag{A.8}$$

Statistically, exchangeability means that the joint distribution remains the same under any permutation of these n random variables. The bracketed expression $\begin{bmatrix} n \\ k \end{bmatrix}$ denotes an unsigned stirling numbers, which count the number of permutations of n objects that contain precisely k cycles. A cycle is a subset of these elements that remains invariant under the permutation. Thus a cyclic permutation on n elements is a permuation with a single cycle, necessarily containing all elements.

As discussed before, the threshold to threshold evolution is governed by two record processes. In terms of the reduced representation of the negative threshold configuration with level i, one has $i-1$ sites that are to the left of $\pi(k^-)$ and the other has $\pi(k^-) - i + 1$ sites that are to its right. Therefore, using Equation A.8, we can write the probability for going from the negative to positive threshold configuration in N steps given that the negative threshold configuration corresponds to $\pi(k^-)$ and has level i,

$$P(N|i, \pi(k^-)) = \sum_{s=1}^{N} \frac{1}{(i-1)!}\begin{bmatrix} i-1 \\ s-1 \end{bmatrix} \frac{1}{(\pi(k^-)-i+1)!}\begin{bmatrix} \pi(k^-)-i+1 \\ N-s \end{bmatrix}. \tag{A.9}$$

This is Equation 3.21.

We can find the Equation A.8 by using the definition of the stirling numbers. Let us consider the system that has $i = 1$. The negative threshold can then be written as

$$\overline{\pi(k^-)} \quad a_1 \quad a_2 \quad ... \quad a_{\pi(k^-)}. \tag{A.10}$$

Configuration A.10 transits by an avalanche into the following configuration,

$$\underline{\pi(k^-)} \quad \overline{a_1} \quad a_2 \quad ... \quad a_{\pi(k^-)}. \tag{A.11}$$

The evolution from this configuration to the positive threshold configuration is a record process. In every record process the first object is a record. The number of avalanches in the threshold to threshold evolution is equal to the number of lower records in the sequence of $\{a_1, a_2, ..., a_{\pi(k^-)}\}$ plus one. The plus one comes from the last avalanche. Therefore, $N-1$ elements of the sequence are records.

Now let us write this records as cycles. The number of permutations of n elements that contains k cycles is given by the Stirling numbers. A given permutation can be represented in many ways. We therefore have to find a canonical representation of permutations with k cycles so that each such permuation can be written in a unique way and thus each representation corresponds to a distinct permutation. This can be done as follows. Firstly, let us write every cycle in a way that the smallest element of it is located at the left of all other elements of that cycle. Then we order this cycles with their left most elements and put all of them next to each other in the same way of their ordering. Therefore, the cycle that is located at the left most place has the greatest left most element. In this way, the number of the records and the cycles are equal. Thus, the number of avalanches in the threshold to threshold evolution is equal to the cycles that are chosen from $\pi(k^-)$ elements plus one. The number of different configurations that have an N step evolution for given $\pi(k^-)$ and $i = 1$ is then given by the unsigned Stirling numbers of the first kind $\left[{\pi(k^-) \atop N-1}\right]$. The number of all possible level 1 reduced configurations with given $\pi(k^-)$ is $\pi(k^-)!$. Therefore, the probability distribution of the number of avalanches in the threshold to threshold evolution is given as

$$P(N|i=1, \pi(k^-)) = \frac{1}{\pi(k^-)!} \left[{\pi(k^-) \atop N-1}\right]. \tag{A.12}$$

Thus, we recover the result in Chapter 3, Equation 3.16.

A.1. Some Useful Identities Involving Stirling Numbers

We use some identities of stirling numbers. First of all, the basic identity that we use is the recurrence relation. It is given in [10] as

$$\begin{bmatrix} n \\ k \end{bmatrix} = (n-1)\begin{bmatrix} n-1 \\ k \end{bmatrix} + \begin{bmatrix} n-1 \\ k-2 \end{bmatrix}. \tag{A.13}$$

The second identity that we use is also given in [10]

$$\frac{1}{n!}\begin{bmatrix} n+1 \\ m+1 \end{bmatrix} = \sum_{k=0}^{n} \frac{1}{k!}\begin{bmatrix} k \\ m \end{bmatrix}. \tag{A.14}$$

The third identity is given in [10] as

$$\sum_{k} \begin{bmatrix} k \\ l \end{bmatrix}\begin{bmatrix} n-k \\ m \end{bmatrix}\binom{n}{l+m} = \begin{bmatrix} n \\ l+m \end{bmatrix}\binom{l+m}{l}, \tag{A.15}$$

The fourth identity is,

$$\sum_{k=0}^{n} \begin{bmatrix} n \\ k \end{bmatrix} = n!. \tag{A.16}$$

The fifth identity is,

$$\sum_{k=0}^{n} x^k \begin{bmatrix} n \\ k \end{bmatrix} = x(x+1)(x+2)...(x+n-1). \tag{A.17}$$

Let us prove identities Equation A.15, Equation A.14. We can simply show Equation A.14 by using the recurrence relation Equation A.13. Let us take the left

hand side of Equation A.14 and expand using Equation A.13,

$$\frac{1}{n!}\begin{bmatrix} n+1 \\ m+1 \end{bmatrix} = \frac{n}{n!}\begin{bmatrix} n \\ m+1 \end{bmatrix} + \frac{1}{n!}\begin{bmatrix} n \\ m \end{bmatrix}. \tag{A.18}$$

Again, use recurrence relation Equation A.13 to expand the first term in Equation A.18

$$\frac{1}{n!}\begin{bmatrix} n+1 \\ m+1 \end{bmatrix} = \frac{n(n-1)}{n!}\begin{bmatrix} n-1 \\ m+1 \end{bmatrix} + \frac{n}{n!}\begin{bmatrix} n-1 \\ m \end{bmatrix} + \frac{1}{n!}\begin{bmatrix} n \\ m \end{bmatrix}. \tag{A.19}$$

If we repeatedly repeat expand the first term n times we find

$$\begin{aligned}\frac{1}{n!}\begin{bmatrix} n+1 \\ m+1 \end{bmatrix} = \frac{n(n-1)...1}{n!}\begin{bmatrix} n-n \\ m+1 \end{bmatrix} \\ + \frac{1}{0!}\begin{bmatrix} 0 \\ m \end{bmatrix} + \frac{1}{1!}\begin{bmatrix} 1 \\ m \end{bmatrix} + ... + \frac{1}{(n-1)!}\begin{bmatrix} n-1 \\ m \end{bmatrix} + \frac{1}{n!}\begin{bmatrix} n \\ m \end{bmatrix}.\end{aligned} \tag{A.20}$$

The first term on the right hand side vanishes, if we choose $m \neq -1$ and we find Equation A.14

$$\frac{1}{n!}\begin{bmatrix} n+1 \\ m+1 \end{bmatrix} = \sum_{k=0}^{n} \frac{1}{k!}\begin{bmatrix} k \\ m \end{bmatrix}. \tag{A.21}$$

A.2. Intermediate Steps leading from Equation A.24 to Equation 3.32

In Chapter 2 we found the following, Equation A.24,

$$P_L(N) = \frac{2^N}{L(L-1)} \sum_{j=1}^{L-2} \frac{(L-j-1)}{j!}\begin{bmatrix} j-1 \\ N-1 \end{bmatrix} + \frac{2}{L}\delta_{N,0}. \tag{A.22}$$

Thus we obtained an expression that contains only one sum. Nevertheless, determining the result of this sum for given N and L is still not so easy, because it involves multiplication of a Stirling number and a factorial. We can simplify this expression further by using some identities involving Stirling numbers. First, we write Equation 3.32

as,

$$P_L(N) = \frac{2^N}{L(L-1)} \sum_{j=1}^{L-2} \left(\frac{(L-1)}{j!} + \frac{j}{j!} \right) \begin{bmatrix} j-1 \\ N-1 \end{bmatrix} + \frac{2}{L}\delta_{N,0}. \tag{A.23}$$

Write Equation A.23 as the part that in the bracket as separately

$$P_L(N) = \frac{2^N}{L(L-1)} \sum_{j=1}^{L-2} \frac{(L-1)}{j!} \begin{bmatrix} j-1 \\ N-1 \end{bmatrix} + \frac{2^N}{L(L-1)} \sum_{j=1}^{L-2} \frac{1}{(j-1)!} \begin{bmatrix} j-1 \\ N-1 \end{bmatrix} + \frac{2}{L}\delta_{N,0}, \tag{A.24}$$

Let us rewrite this expression as,

$$P_L(N) = \Sigma_1 - \Sigma_2 + \frac{2}{L}\delta_{N,0}, \tag{A.25}$$

where,

$$\Sigma_1 = \frac{2^N}{L} \sum_{j=1}^{L-2} \frac{1}{j!} \begin{bmatrix} j-1 \\ N-1 \end{bmatrix},$$
$$\Sigma_2 = \frac{2^N}{L(L-1)} \sum_{j=1}^{L-2} \frac{1}{(j-1)!} \begin{bmatrix} j-1 \\ N-1 \end{bmatrix}.$$

We can easily calculate Σ_2 by using the identity Equation A.14. Therefore, we can write,

$$\begin{aligned} \sum_{j=1}^{L-2} \frac{1}{(j-1)!} \begin{bmatrix} j-1 \\ N-1 \end{bmatrix} &= \sum_{k=0}^{L-3} \frac{1}{k!} \begin{bmatrix} k \\ N-1 \end{bmatrix}, \\ &= \frac{1}{(L-3)!} \begin{bmatrix} L-2 \\ N \end{bmatrix}. \end{aligned} \tag{A.26}$$

So Σ_2 becomes,

$$\Sigma_2 = \frac{2^N}{L(L-1)} \frac{1}{(L-3)!} \begin{bmatrix} L-2 \\ N \end{bmatrix}. \tag{A.27}$$

Now, let us determine Σ_1. With the following change of variables,

$$\begin{aligned} j &\to k+1, \\ N-1 &\to m, \\ L-3 &\to n, \end{aligned}$$

Σ_1 becomes

$$\Sigma_1 = \frac{2^{m+1}}{n+3} \sum_{k=0}^{n} \frac{1}{(k+1)!} \begin{bmatrix} k \\ m \end{bmatrix}. \tag{A.28}$$

Use the recurrence relation Equation A.13 to obtain

$$\begin{bmatrix} n \\ k \end{bmatrix} = (n) \begin{bmatrix} n \\ k+1 \end{bmatrix} - \begin{bmatrix} n+1 \\ k+1 \end{bmatrix}. \tag{A.29}$$

With this identity Σ_1 is written as

$$\Sigma_1 = \frac{2^{m+1}}{n+3} \sum_{k=0}^{n} \frac{1}{(k+1)!} \left(\begin{bmatrix} k+1 \\ m+1 \end{bmatrix} - k \begin{bmatrix} k \\ m+1 \end{bmatrix} \right). \tag{A.30}$$

Add and subtract $\begin{bmatrix} k \\ m+1 \end{bmatrix}$ to the terms in brackets in Equation A.30,

$$\Sigma_1 = \frac{2^{m+1}}{n+3} \sum_{k=0}^{n} \frac{1}{(k+1)!} \left(\begin{bmatrix} k+1 \\ m+1 \end{bmatrix} - (k+1) \begin{bmatrix} k \\ m+1 \end{bmatrix} + \begin{bmatrix} k \\ m+1 \end{bmatrix} \right). \tag{A.31}$$

Write Σ_1 as three separate sums:

$$\Sigma_1 = \frac{2^{m+1}}{n+3} \left(\sum_{k=0}^{n} \frac{1}{(k+1)!} \begin{bmatrix} k+1 \\ m+1 \end{bmatrix} - \sum_{k=0}^{n} \frac{1}{k!} \begin{bmatrix} k \\ m+1 \end{bmatrix} + \sum_{k=0}^{n} \frac{1}{(k+1)!} \begin{bmatrix} k \\ m+1 \end{bmatrix} \right). \tag{A.32}$$

Make change of variable in the first term, $t \equiv k+1$,

$$\sum_{t=1}^{n+1} \frac{1}{t!} \begin{bmatrix} t \\ m+1 \end{bmatrix} = \sum_{t=1}^{n+1} \frac{1}{t!} \begin{bmatrix} t \\ m+1 \end{bmatrix} + \begin{bmatrix} 0 \\ m+1 \end{bmatrix} - \begin{bmatrix} 0 \\ m+1 \end{bmatrix} = \sum_{t=0}^{n+1} \frac{1}{t!} \begin{bmatrix} t \\ m+1 \end{bmatrix} - \begin{bmatrix} 0 \\ m+1 \end{bmatrix}.$$

Use identity, Equation A.14, for both the first and second term in parentheses of Equation A.32. Now Σ_1 becomes,

$$\Sigma_1 = \frac{2^{m+1}}{n+3} \left(\frac{1}{(n+1)!} \begin{bmatrix} n+2 \\ m+2 \end{bmatrix} - \begin{bmatrix} 0 \\ m+1 \end{bmatrix} - \frac{1}{(n)!} \begin{bmatrix} n+1 \\ m+2 \end{bmatrix} + \sum_{k=0}^{n} \frac{1}{(k+1)!} \begin{bmatrix} k \\ m+1 \end{bmatrix} \right). \quad \text{(A.33)}$$

Then, applying the recurrence relation Equation A.13, we have

$$\frac{1}{(n+1)!} \begin{bmatrix} n+2 \\ m+2 \end{bmatrix} - \frac{1}{(n)!} \begin{bmatrix} n+1 \\ m+2 \end{bmatrix} = \begin{bmatrix} n+1 \\ m+1 \end{bmatrix}. \quad \text{(A.34)}$$

Therefore, we can write Σ_1 as,

$$\Sigma_1 = \frac{2^{m+1}}{n+3} \left(\frac{1}{(n+1)!} \begin{bmatrix} n+1 \\ m+1 \end{bmatrix} - \begin{bmatrix} 0 \\ m+1 \end{bmatrix} + \sum_{k=0}^{n} \frac{1}{(k+1)!} \begin{bmatrix} k \\ m+1 \end{bmatrix} \right). \quad \text{(A.35)}$$

If we look at the difference between Equation A.28 and Equation A.35, we see that,

$$\sum_{k=0}^{n} \frac{1}{(k+1)!} \begin{bmatrix} k \\ m \end{bmatrix} = \frac{1}{(n+1)!} \begin{bmatrix} n+1 \\ m+1 \end{bmatrix} - \begin{bmatrix} 0 \\ m+1 \end{bmatrix} + \sum_{k=0}^{n} \frac{1}{(k+1)!} \begin{bmatrix} k \\ m+1 \end{bmatrix}. \quad \text{(A.36)}$$

If we use Equation A.36 to expand the last term in the same equation we find

$$\sum_{k=0}^{n} \frac{1}{(k+1)!} \begin{bmatrix} k \\ m \end{bmatrix} = \frac{1}{(n+1)!} \begin{bmatrix} n+1 \\ m+1 \end{bmatrix} - \begin{bmatrix} 0 \\ m+1 \end{bmatrix} + \frac{1}{(n+1)!} \begin{bmatrix} n+1 \\ m+2 \end{bmatrix} - \begin{bmatrix} 0 \\ m+2 \end{bmatrix} + \sum_{k=0}^{n} \frac{1}{(k+1)!} \begin{bmatrix} k \\ m+2 \end{bmatrix}. \quad \text{(A.37)}$$

Let us repeat this process p times until the last term in the equation vanishes. It will vanish if all terms in the sum vanishes. Therefore, $m+p$ must be greater than the

maximum value that k can take which is n. After repeating this process $p = n-m+1$ times, our expression becomes,

$$\sum_{k=0}^{n} \frac{1}{(k+1)!} \begin{bmatrix} k \\ m \end{bmatrix} = \sum_{p=1}^{n-m+1} \frac{1}{(n+1)!} \begin{bmatrix} n+1 \\ m+p \end{bmatrix} - \sum_{p=1}^{n-m+1} \begin{bmatrix} 0 \\ m+p \end{bmatrix}. \tag{A.38}$$

With this identity, Σ_1 can be written as,

$$\Sigma_1 = \frac{2^{m+1}}{n+3} \left(\sum_{p=1}^{n-m+1} \frac{1}{(n+1)!} \begin{bmatrix} n+1 \\ m+p \end{bmatrix} - \sum_{p=1}^{n-m+1} \begin{bmatrix} 0 \\ m+p \end{bmatrix} \right), \tag{A.39}$$

Change the variables back to their initial versions,

$$\begin{aligned} k &\to j-1, \\ m &\to N-1, \\ n &\to L-3. \end{aligned}$$

Therefore, Σ_1 becomes,

$$\Sigma_1 = \frac{2^N}{L} \left(\sum_{p=1}^{L-N-1} \frac{1}{(L-2)!} \begin{bmatrix} L-2 \\ N-1+p \end{bmatrix} - \sum_{p=1}^{L-N-1} \begin{bmatrix} 0 \\ N-1-p \end{bmatrix} \right). \tag{A.40}$$

Also change the p variable, $p \to t-N+1$,

$$\pi_1 = \frac{2^N}{L} \left(\sum_{t=N}^{L-2} \frac{1}{(L-2)!} \begin{bmatrix} L-2 \\ t \end{bmatrix} - \sum_{t=N}^{L-2} \begin{bmatrix} 0 \\ t \end{bmatrix} \right). \tag{A.41}$$

Now, let us substitute Σ_1 and Σ_2, Equation A.41 and Equation A.27, into Equation A.25,

$$\begin{aligned} P_L(N) = \frac{2^N}{L} \left(\sum_{t=N}^{L-2} \frac{1}{(L-2)!} \begin{bmatrix} L-2 \\ t \end{bmatrix} - \sum_{t=N}^{L-2} \begin{bmatrix} 0 \\ t \end{bmatrix} \right) \\ - \frac{2^N}{L(L-1)} \frac{1}{(L-3)!} \begin{bmatrix} L-2 \\ N \end{bmatrix} + \frac{2}{L} \delta_{N,0} \end{aligned} \tag{A.42}$$

Let us arrange the terms as follow

$$P_L(N) = \frac{2^N}{L!} \underbrace{\left((L-1) \sum_{t=N}^{L-2} \begin{bmatrix} L-2 \\ t \end{bmatrix} - (L-2) \begin{bmatrix} L-2 \\ N \end{bmatrix} \right)}_{\mathbf{A}} - \frac{2^N}{L} \sum_{t=N}^{L-2} \begin{bmatrix} 0 \\ t \end{bmatrix} + \frac{2}{L} \delta_{N,0}. \quad \text{(A.43)}$$

We can find a simplified version of expression **A** in Equation A.43. First write **A** as

$$\mathbf{A} = \sum_{t=N}^{L-2} (L-2) \begin{bmatrix} L-2 \\ t \end{bmatrix} + \sum_{t=N}^{L-2} \begin{bmatrix} L-2 \\ t \end{bmatrix} - (L-2) \begin{bmatrix} L-2 \\ N \end{bmatrix}. \quad \text{(A.44)}$$

Next use recurrence relation, Equation A.13 for the first term in Equation A.44

$$\mathbf{A} = \sum_{t=N}^{L-2} \left(\begin{bmatrix} L-1 \\ t \end{bmatrix} - \begin{bmatrix} L-2 \\ t-1 \end{bmatrix} \right) + \sum_{t=N}^{L-2} \begin{bmatrix} L-2 \\ t \end{bmatrix} - (L-2) \begin{bmatrix} L-2 \\ N \end{bmatrix}, \quad \text{(A.45)}$$

and regroup the sums

$$\mathbf{A} = \sum_{t=N}^{L-2} \begin{bmatrix} L-1 \\ t \end{bmatrix} + \sum_{t=N}^{L-2} \left(\begin{bmatrix} L-2 \\ t \end{bmatrix} - \begin{bmatrix} L-2 \\ t-1 \end{bmatrix} \right) - (L-2) \begin{bmatrix} L-2 \\ N \end{bmatrix}. \quad \text{(A.46)}$$

All terms in the second sum vanish except for the two terms below:

$$\mathbf{A} = \sum_{t=N}^{L-2} \begin{bmatrix} L-1 \\ t \end{bmatrix} + \begin{bmatrix} L-2 \\ L-2 \end{bmatrix} - \begin{bmatrix} L-2 \\ N-1 \end{bmatrix} - (L-2) \begin{bmatrix} L-2 \\ N \end{bmatrix}. \quad \text{(A.47)}$$

Use the recurrence relation, Equation A.13, again for the last two term and noting that $\begin{bmatrix} n \\ n \end{bmatrix} = 1$,

$$\mathbf{A} = \sum_{t=N}^{L-2} \begin{bmatrix} L-1 \\ t \end{bmatrix} + \begin{bmatrix} L-1 \\ L-1 \end{bmatrix} - \begin{bmatrix} L-1 \\ N \end{bmatrix}, \quad \text{(A.48)}$$

where Equation A.48 can be written as

$$\mathbf{A} = \sum_{t=N+1}^{L-1} \begin{bmatrix} L-1 \\ t \end{bmatrix}. \tag{A.49}$$

Substitute Equation A.49 into Equation A.43,

$$P_L(N) = \frac{2^N}{L!} \sum_{t=N+1}^{L-1} \begin{bmatrix} L-1 \\ t \end{bmatrix} - \frac{2^N}{L} \sum_{t=N}^{L-2} \begin{bmatrix} 0 \\ t \end{bmatrix} + \frac{2}{L}\delta_{N,0}. \tag{A.50}$$

Finally note that $\begin{bmatrix} 0 \\ k \end{bmatrix} = 0$ for $k > 0$ and $\begin{bmatrix} 0 \\ 0 \end{bmatrix} = 1$ and $N \geq 0$, thus the second sum gives a non-zero contribution only when $N = 0$. Therefore,

$$\begin{aligned} P_L(N) &= \frac{2^N}{L!} \sum_{t=N+1}^{L-1} \begin{bmatrix} L-1 \\ t \end{bmatrix} - \frac{2^0}{L}\delta_{N,0} + \frac{2}{L}\delta_{N,0}, \\ &= \frac{2^N}{L!} \sum_{t=N+1}^{L-1} \begin{bmatrix} L-1 \\ t \end{bmatrix} + \frac{1}{L}\delta_{N,0}. \end{aligned} \tag{A.51}$$

Equation A.51 gives the probability distribution of number of avalanches in the threshold to threshold evolution.

REFERENCES

1. Middleton, A. and D. Fisher, "Critical Behavior of Charge-Density Wave Below Threshold: Numerical and Scaling Analysis", *Physical Review B*, Vol. 47, p. 3530, 1993.

2. Sethna, J., K. Dahmen, S. Kartha, J. Krumhansl, B. Roberst and J. Shore, "Hysteresis And Hierarchies: Dynamics Of Disorder-Driven First-Order Phase Transformations", *Physical Review Letter*, Vol. 70, p. 3347, 1993.

3. Fisher, D., "Threshold Behavior of Charge-Density Waves Pinned by Impurities", *Physical Review Letter*, Vol. 50, p. 1486, 1983.

4. Fisher, D., "Sliding Charge-Density Waves As a Dynamic Critical Phenomenon", *Physical Review B*, Vol. 31, p. 1396, 1985.

5. Fukuyarna, H. and P. Lee, "Dynamics Of The Charge-Density Wave. I. Impurity Pinning In A Single Chain", *Physical Reiew B*, Vol. 17, p. 535, 1978.

6. Lee, P. and T. Rice, "Electric Field Depinning Of Charge Density Waves", *Physical Review B*, Vol. 19, p. 3970, 1979.

7. Landsberg, A. and E. Friedman, "Dynamical Effects Of Partial Orderings In Physical Systems", *Physical Review E*, Vol. 54, p. 3135, 190.

8. Kaspar, D. and M. Mungan, "Subthreshold Behavior and Avalanches In An Exactly Solvable Charge Density Wave System", *arXiv:1304.2845*, 2013.

9. Arnold, N. B. B. and H. Nagaraja, *Records*, Wiley, 1998.

10. Graham, R., D. Knuth and O. Patashnik, *Concrete Mathematics: A Foundation for Computer Science*, Addison-Wesley, 1994.